Total evidence phylogeny of platyrrhine primates and a comparison of undated and tip-dating approaches

Robin M. D. Beck [a,*], Dorien de Vries [a], Mareike C. Janiak [a], Ian B. Goodhead [a], Jean P. Boubli [a]

[a] *Ecosystems and Environment Research Centre, School of Science, Engineering and Environment, University of Salford, Manchester, UK*

*__Corresponding author__.

E-mail address: r.m.d.beck@salford.ac.uk (R. M. D. Beck)

Total evidence phylogeny of platyrrhine primates and a comparison of undated and tip-dating approaches

Abstract

There have been multiple published phylogenetic analyses of platyrrhine primates (New World monkeys) using both morphological and molecular data, but relatively few that have integrated both types of data into a total evidence approach. Here, we present phylogenetic analyses of Recent and fossil platyrrhines, based on a total evidence dataset of 418 morphological characters and 10.2 kilobases of DNA sequence data from 17 nuclear genes taken from previous studies, using undated and tip-dating approaches in a Bayesian framework. We compare the results of these analyses with molecular scaffold analyses using maximum parsimony and Bayesian approaches, and we use a formal information theoretic approach to identify unstable taxa. After a posteriori pruning of unstable taxa, the undated and tip-dating topologies appear congruent with recent molecular analyses and support largely similar relationships, with strong support for *Stirtonia* as a stem alouattine, *Neosaimiri* as a stem saimirine, *Cebupithecia* as a stem pitheciine, and *Lagonimico* as a stem callitrichid. Both analyses find three Greater Antillean subfossil platyrrhines (*Xenothrix*, *Antillothrix*, and *Paralouatta*) to form a clade that is related to *Callicebus*, congruent with a single dispersal event by the ancestor of this clade to the Greater Antilles. They also suggest that the fossil *Proteropithecia* may not be closely related to pitheciines, and that all known platyrrhines older than the Middle Miocene are stem taxa. Notably, the undated analysis found the Early Miocene *Panamacebus* (currently recognized as the oldest known cebid) to be unstable, and the tip-dating analysis placed it outside crown

Platyrrhini. Our tip-dating analysis supports a late Oligocene or earliest Miocene (20.8–27.0 Ma) age for crown Platyrrhini, congruent with recent molecular clock analyses.

Keywords: South America; Central America; Greater Antilles; Molecular scaffold; Bayesian; systematics; Divergence times

1. Introduction

Today, the New World monkeys comprise >170 extant species from South and Central America and Mexico (Mammal Diversity Database, 2020). They are classified into as many as five families (‘IUCN/SSC Primate Specialist Group—Taxonomy,’ n.d.; Schneider and Sampaio, 2015; Mammal Diversity Database, 2020): Atelidae (howler monkeys, spider monkeys, and relatives), Pitheciidae (titis, sakis, and uakaris), Cebidae (squirrel monkeys and capuchins), Callitrichidae (marmosets and tamarins) and Aotidae (night or owl monkeys), with the last two considered to be subfamilies within Cebidae in some classifications (e.g., Kay, 2015; Rosenberger, 2020). These five families are members of the clade Platyrrhini, which among living primates is sister to Catarrhini (apes and Old World monkeys; e.g., Perelman et al., 2011; Springer et al., 2012; dos Reis et al., 2018). There is a fragmentary but steadily improving record of fossil and subfossil primates from Central and South America and the Greater Antilles (Cooke et al., 2011; Rosenberger et al., 2011; Bond et al., 2015; Kay, 2015; Bloch et al., 2016; Marivaux et al., 2016a, b, 2020a; Halenar et al., 2017; Novo et al., 2017, 2021; Kay and Perry, 2019; Kay et al., 2019; Rosenberger, 2020; Seiffert et al., 2020; Antoine et al., 2021; Fleagle et al., 2022), dating from the late Eocene (Antoine et al., 2021) or early Oligocene (Campbell et al., 2021) onwards; most of these have been confidently identified as either stem or crown platyrrhines, but

there are some notable exceptions, most obviously the parapithecid (=stem anthropoid) *Ucayalipithecus perdita* (Seiffert et al., 2020).

Recent molecular studies appear to have robustly resolved most higher-level relationships among extant platyrrhines, consistently recovering the monophyly of the five Recent families, and placing Pitheciidae as sister to the remaining families, with Cebidae, Callitrichidae, and Aotidae forming a clade to the exclusion of Atelidae (Perelman et al., 2011; Springer et al., 2012; dos Reis et al., 2018). DNA sequence data is also available for the subfossil taxon *Xenothrix mcgregori* from the Quaternary of Jamaica, and suggest that, among extant platyrrhine genera, *Xenothrix* is most closely related to the callicebine pitheciid *Cheracebus* (Woods et al., 2018). However, the precise branching relationship between Cebidae, Callitrichidae, and Aotidae remains uncertain, even with very large molecular datasets (Schrago and Seuánez, 2019; Vanderpool et al., 2020).

Molecular data are currently unavailable for fossil and (with the exception of *Xenothrix*) subfossil members of Platyrrhini, as well as for other fossil primates more than ~2 million years old (Welker et al., 2019, 2020); thus, inclusion of such fossil taxa in phylogenetic analyses requires morphological data. However, published morphology-only analyses of platyrrhines show several areas of disagreement with the current molecular consensus: for example, unconstrained analysis of the craniodental matrix of Kay et al. (2008) failed to recover monophyly of Cebidae or Pitheciidae, and found relationships within Callitrichidae that differ markedly from those supported by molecular data (Kay et al., 2008, their fig. 21). Most recent phylogenetic analyses of platyrrhines that have used morphological data have therefore enforced a ‘molecular scaffold’ that constrains relationships among extant taxa to match the current molecular consensus (Kay, 2015; Bloch et al., 2016; Marivaux et al., 2016a; Kay et al., 2019).

However, such molecular scaffold analyses do not allow synergistic interaction between morphological and molecular data (Hermsen and Hendricks, 2008). Specifically, when morphological data are analyzed with a molecular scaffold, the morphological data cannot overturn the relationships between the taxa in the scaffold, while the positions of the taxa not in the scaffold (which are free to move anywhere in the tree) are determined by morphological data alone (although the molecular scaffold has an indirect effect by influencing the optimization of the morphological character states; Hermsen and Hendricks, 2008).

An alternative is to use a total evidence approach, in which morphological and molecular data are combined and analyzed simultaneously, without the need for topological constraints. Because both data types have an influence on all nodes in the tree, the total evidence approach has been argued by multiple researchers to be the most rigorous (or assumption-free) method for combining morphological and molecular data (e.g., de Queiroz and Gatesy, 2007; Manos et al., 2007; Dávalos et al., 2014; Darlim et al., 2022). However, total evidence analyses are computationally much more demanding than equivalent molecular scaffold analyses (Lee and Palci, 2015), and they require familiarity with both data types and with the methods and software available to analyze them.

In terms of characters, modern molecular sequence datasets are typically far larger (often by a factor of 100 or more) than taxonomically equivalent morphological datasets, and so it has been argued that the phylogenetic signal present in the morphological data will inevitably be overwhelmed by that in the molecular data when these datasets are combined and analyzed simultaneously; if so, a total evidence analysis might be expected to recover the same topology as the equivalent molecular scaffold analysis (Lee and Palci, 2015; Darlim et al., 2022). However, it has been shown that morphological data can influence tree topology even when

combined with much larger molecular datasets (Neumann et al., 2021), and equivalent total evidence and molecular scaffold analyses often show topological differences, particularly in terms of the relationships of taxa unrepresented by molecular data, which include (in the absence of ancient DNA or paleoproteomic data) all fossil taxa (Asher et al., 2005; Hermsen and Hendricks, 2008; Chen et al., 2019). This may be due, at least in part, to the presence of secondary signals in the morphological and/or molecular data that only emerge when analyzed together (Gatesy et al., 1999; Hermsen and Hendricks, 2008), and so remain concealed in a molecular scaffold analysis. More generally, even when morphological and molecular data support very different topologies when analyzed separately, clades recovered in a total evidence analysis are often found to receive support from both data types (e.g., Gatesy et al., 1999, 2003; Lee and Camens, 2009), providing further justification for combining both data types and analyzing them simultaneously.

One argument in favor of use of molecular scaffold analysis over total evidence analysis is that the latter might be negatively impacted by the large amounts of missing data present when some taxa are represented by morphological data only (Manos et al., 2007). However, numerous studies suggest that large amounts of missing data are not necessarily problematic for phylogenetic inference (Wiens and Moen, 2008; Wiens and Tiu, 2012; Mongiardino Koch et al., 2021), including when using a total evidence approach (Wiens, 2009; Guillerme and Cooper, 2016), and total evidence analyses are often equally or better resolved than equivalent molecular scaffold analyses (e.g., Asher et al., 2005: fig. 9; Manos et al., 2007). Some studies have suggested that Bayesian, model-based methods—which are increasingly widely used for total evidence analyses (e.g., Ronquist et al., 2012a; Beck and Lee, 2014; Herrera and Dávalos, 2016; Zhang et al., 2016; Lee and Yates, 2018; Beck and Taglioretti, 2020; Beck et al., 2022; Heritage

and Seiffert, 2022)—suffer specific negative impacts caused by missing data in comparison to maximum parsimony (Goloboff and Pol, 2005; Simmons, 2014; King, 2019). However, subsequent work suggests that, in practice, such negative impacts are unlikely to be particularly problematic (King, 2021:289–290; Mongiardino Koch et al., 2021), and the simulation study of Mongiardino Koch et al. (2021) found that in fact the accuracy of maximum parsimony is more adversely affected by missing data than is Bayesian inference. In addition, it is clear that maximum parsimony analysis of molecular sequence data can lead to the recovery of strongly supported but incorrect topologies (Holder and Lewis, 2003; Yang and Rannala, 2012). Model-based inference (whether in a maximum likelihood or Bayesian framework) will undoubtedly become the standard method for analyzing total evidence datasets; such an approach will allow the use of increasingly sophisticated, biologically more realistic models for both molecular and morphological data, and (where relevant) fossil sampling (e.g., Wright et al., 2016; Pyron, 2017; Andréoletti et al., 2022; Ogilvie et al., 2022).

One form of analysis that is increasingly widely used with total evidence data is ‘tip dating’, in which the ages of the terminal taxa (i.e., tips) help determine branching pattern in combination with the character data, in the context of a single analysis; estimates of divergence times are also calculated (Pyron, 2011; Ronquist et al., 2012a; O’Reilly et al., 2015; Zhang et al., 2016; Lee, 2020; King, 2021). Such analyses do not require prior assumptions regarding the relationships of either the extant or fossil taxa included, and so they may (in principle) be preferable to the usual approach for calibrating divergence times in molecular clock studies, namely ‘node-dating’, which requires that the relationships of fossil taxa are assumed a priori in order to place constraints on the ages of particular nodes (Benton et al., 2015; dos Reis et al., 2016). Importantly, the temporal information incorporated into a tip-dating analysis directly

influences tree topology, not just divergence times, and so undated and tip-dating analyses of the same character data can result in quite different trees (King et al., 2017; Turner et al., 2017; Lee and Yates, 2018; Beck and Taglioretti, 2020; King and Beck, 2020; King, 2021; Heritage and Seiffert, 2022). Whether this is a strength or a weakness of tip dating is debated (King et al., 2017; Turner et al., 2017; Lee and Yates, 2018; King, 2021), but a recent simulation study found that tip-dating analyses generally outperformed equivalent undated analyses, although this effect diminished as the amount of missing data increased (Mongiardino Koch et al., 2021).

It is possible to carry out tip dating using a molecular scaffold approach, in which case divergence times are determined solely by the morphological data (i.e., a morphological clock), as was done by Schrago et al. (2013) for platyrrhines. However, it seems likely that simultaneous analysis of morphological and molecular data (i.e., a total evidence clock) will result in more accurate estimates of divergence times, because molecular data has been shown to evolve in a much more 'clock-like' manner than morphological data (e.g., Beck and Lee, 2014; dos Reis et al., 2016; Kittel et al., 2016; Klopfstein et al., 2019; Cascini et al., 2019).

Despite the seeming advantages of a total evidence approach, there have been relatively few such analyses focusing on platyrrhine relationships. We remedy this here by combining an existing 418-character morphological dataset specifically designed for resolving platyrrhine phylogeny (taken from Kay et al. 2019) with 10.2 kilobases (kb) of existing DNA sequence data from 17 nuclear loci, to formally test the relationships of extant platyrrhines and a range of fossil relatives in a total evidence context. We present Bayesian undated analyses of the molecular and morphological datasets individually, and we carry out Bayesian undated and tip-dating analyses of the total evidence matrix. For the purposes of comparison with previous studies (Kay et al., 2008, 2019; Kay, 2015; Bloch et al., 2016; Marivaux et al., 2016a), we also carry out maximum

parsimony analysis of the morphological dataset, both with and without a molecular scaffold, and also a Bayesian analysis of the morphological dataset with a molecular scaffold. For each analysis, we use objective information-theoretic approaches to identify unstable taxa. Most notably, our tip-dating total evidence analysis recovers several novel relationships, which have important implications for the age of crown Platyrrhini and for the biogeography of the group. We also identify which currently known fossil platyrrhines are suitable for use as calibrations for node-dating analyses. Our study provides further insight into platyrrhine phylogeny, identifying which fossil taxa have robustly resolved relationships and which are unstable, and also provides a new estimate of divergence times within the clade.

2. Methods

2.1. Dataset preparation

Our molecular dataset comprises DNA sequences from 17 nuclear loci that were selected based on their availability for our extant taxon sample and also for the Jamaican subfossil *Xenothrix* (Perelman et al., 2011; Springer et al., 2012; Woods et al., 2018); these sequences were downloaded from Genbank (https://www.ncbi.nlm.nih.gov/genbank/), aligned using MUSCLE (Edgar, 2004) with default settings in MEGA v. 10.2.6 (Kumar et al., 2018), and concatenated into a single file, resulting in a total of 10244 base pairs of sequence data (Table 1); of these, 1679 (=16.4%) are variable, with 673 (=6.6%) parsimony informative and 1006 (=9.8%) autapomorphic. Our morphological dataset is that of Kay et al. (2019), which comprises 418 characters from the dentition, cranium, postcranium, and soft tissues, of which 348 (=83.3%) are variable, with 314 (=75.1%) parsimony informative and 34 (=8.1%) autapomorphic; of these 418,175 (=41.9%) represent putative morphoclines that have been ordered here. Because

MrBayes v. 3.2.7a does not allow weighting of characters, we did not scale the weights of ordered morphological characters according to the number of states (contra Kay et al., 2019; see also Kay et al., 2008) but instead assigned each morphological character equal weight. The phylogenetic analyses of Bloch et al. (2016), who used a very similar morphological dataset, show that the major impact of equal weighting is a loss of resolution, with relationships that were present but weakly supported in the weighted analysis collapsing in the equally weighted analysis (compare Supplementary Figures 5 and 7 with Supplementary Figures 6 and 8 of Bloch et al., 2016). Kay et al. (2019) scored these characters for 16 extant platyrrhine genera, 24 fossil and subfossil primate taxa from South and Central America and the Greater Antilles, three extant catarrhine genera (*Hylobates*, *Miopithecus* and *Presbytis*), and five fossil anthropoids from Africa (*Apidium*, *Aegyptopithecus*, *Catopithecus*, *Proteopithecus* and *Simonsius*). To make our total evidence dataset, the morphological and aligned molecular datasets were merged into a single matrix. Our molecular, morphological, and total evidence matrices (including the relevant TNT and MrBayes commands required to run each analysis, see below), can be found in Supplementary Online Material (SOM).

2.2. Maximum parsimony analyses

For this study, we specifically focus on the results of our total evidence analyses, for reasons discussed in our Introduction. However, for the purposes of comparison, and because several recent studies of platyrrhine phylogeny have used maximum parsimony (MP) analysis with a molecular scaffold (Kay, 2015; Bloch et al., 2016; Marivaux et al., 2016a; Kay et al., 2019), we also carried out MP analysis of the morphological dataset, with and without the use of a molecular scaffold. We did not undertake MP analyses of our molecular or total evidence

datasets, given that model-based approaches have consistently been shown to outperform MP when analyzing molecular sequence data (see Introduction). MrBayes v. 3.2.7a treats all cases of polymorphism as missing data. Therefore, to maximize comparability between analyses, we also specified polymorphisms (433 out of 11,975 total character scores, or 3.6%) as missing data in our MP analyses. The MP analyses were implemented in TNT v. 1.5 (Goloboff et al., 2008; Goloboff and Catalano, 2016), running on a Windows 10 PC, and comprised a 'New Technology' search with Sectorial Search, Ratchet, Drift, and Tree Fusing that was run until the same minimum tree length was found 100 times, followed by a 'Traditional' search with tree bisection reconnection within the trees saved from the first search. Multiple most parsimonious trees (where present) were summarized using strict consensus. Support values for clades present in the strict consensus were calculated using 2000 bootstrap replicates, again with traditional search, with the results output as absolute frequencies. Following Hillis and Bull (1993), we considered bootstrap values ≥70% to represent strong support, and bootstrap values 50–69% to represent moderate support.

Initial MP analyses of the morphological dataset without any topological constraints, and with *Proteopithecus* specified as the outgroup, recovered the parapithecids *Apidium* and *Simonsius* within crown Anthropoidea, as stem catarrhines (data not shown). However, parapithecids are widely accepted to be stem anthropoids, and recent phylogenetic analyses of broadscale primate relationships consistently place both *Apidium* and *Simonsius* outside crown Anthropoidea (e.g., Jaeger et al., 2019; Morse et al., 2019; Ni et al., 2019; Seiffert et al., 2020). The topology found here is likely because this morphological dataset was intended to resolve relationships within Platyrrhini, and taxa (e.g., *Qatrania*) and characters relevant to resolving the relationships of parapithecids have not been included (see comments by Kay et al., 2008:350).

The Kay et al. (2019) dataset includes two South American taxa with uncertain relationships to Platyrrhini, namely *Perupithecus* and *Parvimico* (Bond et al., 2015; Kay et al., 2019; Wisniewski et al., 2022). To ensure correct character polarities at the base of the tree, which should help place *Perupithecus* and *Parvimico*, we therefore applied a topological constraint that forced *Proteopithecus*, *Apidium*, and *Simonsius* to fall outside a clade comprising our remaining taxa. For the tip-dating analysis of our total evidence dataset, we calibrated the ages of crown Catarrhini (=*Hylobates* + *Miopithecus* + *Presbytis*) and crown Cercopithecidae (=*Miopithecus* + *Presbytis*), which required that these clades were constrained as monophyletic (see below); to maximize comparability between analyses, we also specified these two constraints in our maximum parsimony analysis, but we note that, in any case, both clades were recovered with strong (≥85%) bootstrap support when topological constraints were not applied (data not shown). We do not present support values for the three constrained clades in any of our analyses because their monophyly was enforced a priori, and hence support values for these clades are meaningless.

The MP analysis with a molecular scaffold enforced the same backbone constraint used by Kay et al. (2019), but with *Proteopithecus*, *Apidium*, and *Simonsius* added at the base, for the reasons explained above. Support values for clades present in the strict consensus from this analysis were again calculated using 2000 bootstrap replicates with traditional search, with the results output as absolute frequencies, and with bootstrap values ≥70% considered as strong support, and bootstrap values 50–69% as moderate support.

2.3. Bayesian analyses

All our Bayesian phylogenetic analyses were carried out using MrBayes v. 3.2.7a (Huelsenbeck and Ronquist, 2001; Ronquist et al., 2012b), running on the JASMIN, the UK's collaborative data analysis environment (https://jasmin.ac.uk; Lawrence et al., 2013). Although our focus is undated and tip-dating analysis of the total evidence dataset, we also carried out Bayesian undated analyses of the morphological and molecular datasets individually, and also a Bayesian undated analysis of the morphological dataset with a molecular scaffold, to compare topologies and assess relative phylogenetic signal between the two datasets, and to allow comparison with our MP analyses (see above) and with previous phylogenetic analyses of platyrrhines, most of which have used MP analysis of morphological data with a molecular scaffold (Kay et al., 2008, 2019; Kay, 2015; Bloch et al., 2016; Marivaux et al., 2016a).

For the molecular dataset, PartitionFinder v. 2.2 (Lanfear et al., 2017) was first used to identify an appropriate partitioning scheme (with the alignment initially partitioned by gene) and substitution model for each partition, with possible models restricted to only those implemented by MrBayes; model variants that combine a gamma distribution to model rate heterogeneity between sites with a proportion of invariant sites were not considered, following the recommendations of Stamatakis (2014). The PartitionFinder analysis used the ‘greedy algorithm’ and assumed linked branch lengths, and the Bayesian Information Criterion (BIC) was used for model selection. The best fitting partitioning scheme and set of substitution models are shown in Table 1. Because we did not consider models that combine a gamma distribution and a proportion of invariant sites, we increased the number of gamma rate categories from the MrBayes default of four to eight.

Given the comparatively large number of autapomorphies (34 out of 348 variable characters = 9.8%) in the morphological dataset (which may be particularly important for tip-

dating; Lee, 2020), we assigned it the Lewis (2001) Mk substitution model with the assumption that variable characters have been scored, i.e. the Mk*v* variant (the 70 constant characters were therefore ignored in the analysis), with an eight category lognormal distribution to model rate heterogeneity between sites (Harrison and Larsson, 2015).

<TABLE 1 ABOUT HERE>

For undated analysis of the molecular dataset, we did not assume any topological constraints, and we assumed linked branch lengths between all partitions. MrBayes settings for this analysis comprised two independent runs of four Markov Chain Monte Carlo (MCMC) chains (one 'cold', three 'heated', with default heating parameters), run for 5×10^6 generations and sampling trees and other parameters every 5000 generations. Use of Tracer v. 1.7 (Rambaut et al., 2018) indicated that stationarity and convergence between runs was achieved within 5 x 10^5 generations; based on this, the first 10% of sampled trees were excluded (leaving 900 post-burnin trees for each run). The post-burnin trees were summarized in MrBayes using 50% majority rule consensus (following the recommendations of O'Reilly and Donoghue, 2018). Support values were calculated as Bayesian posterior probabilities (BPPs); we consider BPP 0.5–0.74 as weak support, 0.75–0.94 as moderate support, and 0.95–1.00 as strong support (Alfaro et al., 2003).

In all our Bayesian morphological and total evidence analyses, we forced *Proteopithecus*, *Apidium*, and *Simonsius* to fall outside a clade comprising our remaining taxa, and we enforced monophyly of crown Catarrhini and crown Cercopithecidae, the same as in our MP analyses (see

above). For our morphological analysis with a molecular scaffold, we enforced the same backbone constraint used by Kay et al. (2019), but with *Proteopithecus*, *Apidium*, and *Simonsius* added at the base, again the same as in the equivalent MP analysis (see above).

MrBayes settings for the undated morphological analysis, with and without a molecular scaffold, were the same as for the undated molecular analysis. Stationarity and convergence between runs were achieved within 5×10^5 generations; based on this, the first 10% of sampled trees were excluded (leaving 900 post-burnin trees for each run), and the post-burnin trees were summarized as above. For undated analysis of the total evidence dataset, we unlinked branch lengths between the morphological and molecular partitions, because these partitions should be expected to show very different relative branch lengths (which are proportional to the estimated amount of change per character; Barba-Montoya et al., 2021; Mather et al., 2021), but linked them between molecular partitions (as in the undated molecular analysis). MrBayes settings for these analyses were the same as for the undated morphological and molecular analyses, except that it was run for 10×10^6 generations. Stationarity and convergence between runs were achieved within 5×10^6 generations; based on this, the first 50% of sampled trees were excluded (leaving 1000 post-burnin trees for each run), and the post-burnin trees were summarized as above.

For the tip-dating analysis of the total evidence dataset, branch lengths were linked across morphological and molecular partitions to produce a single set of branch lengths that were proportional to time. We assigned a fixed age of 0 Ma to all of our extant taxa. For our fossil and subfossil taxa, we assigned ages based on the recent literature; in all cases, we have based these on radiometric and/or magnetostratigraphic dates, even when these provide only relatively loose age constraints (Table 2), as we consider that these are likely to be more reliable than those based

on biostratigraphy (see e.g., Kay et al., 1999). In most cases, we assigned a uniform age prior corresponding to the entire possible age range of the specimens used for scoring purposes (following Püschel et al., 2020). However, we assigned a fixed age of 33.4 Ma to *Catopithecus* and *Proteopithecus*, all specimens of which are from Quarry L-41 of the Jebel Qatrani Formation in the Fayum Depression of Egypt, which has been assigned an age of 33.4 Ma by Van Couvering and Delson (2020). A full justification of the assigned ages for all of our fossil and subfossil taxa is given in Table 2. We assigned age constraints on two internal nodes based on calibrations suggested by de Vries and Beck (2021): specifically, we enforced a uniform constraint on the age of crown Catarrhini with a hard minimum bound of 25.193 Ma and a hard maximum bound of 33.4 Ma, and an offset exponential constraint on the age of crown Cercopithecidae with a hard minimum bound of 12.47 Ma and a soft maximum bound of 25.235 Ma (see de Vries and Beck, 2021, for full details). Following Sallam and Seiffert (2020), we also calibrated the age of the root as a truncated normal prior with a minimum of 33.401 Ma (which is only slightly older than the oldest taxa in our dataset, namely *Catopithecus* and *Proteopithecus*—see above), a mean age that is 0.1 Ma older than the age of our oldest fossil taxa (i.e., 33.5 Ma), and a standard deviation of 1.0 Ma.

<TABLE 2 ABOUT HERE>

We applied a single independent gamma rates (IGR) clock model to the entire molecular partition, and a separate IGR model to the morphological partition, with the prior on the clock rate specified using the custom R script of Gunnell et al. (2018), and the prior on the variance left as the MrBayes default. For the tree model, we assumed the fossilized birth-death (FBD) process

(Stadler, 2010; Gavryushkina et al., 2014; Heath and Huelsenbeck, 2014), allowing for sampled ancestors, and with diversity sampling assumed (Zhang et al., 2016). Because our focus is Platyrrhini, and our taxa are genus-level (with one possible exception, '*Aotus*' *dindensis*, which nevertheless does not form a clade with extant *Aotus* in several recent phylogenetic analyses, and has been argued to be conspecific with *Mohanamico hershkovitzi*, hence our use of quotation marks; Kay, 2015; Marivaux et al., 2016a; Kay et al., 2019; but see Ni et al., 2019), we assumed a sampling probability of 0.727, corresponding to the inclusion of 16 of the 22 extant platyrrhine genera currently recognized. Priors on speciation, extinction, and sampling were left as the MrBayes defaults.

Settings for the MrBayes runs were the same as for the previous analyses, except that the analysis was run for 40 x 10^6 generations. Stationarity and convergence between runs were achieved within 4 x 10^6 generations; based on this, the first 10% of sampled trees were excluded (leaving 7200 post-burnin trees for each run). The post-burnin trees were initially summarized in MrBayes using 50% majority rule consensus. However, lack of resolution in a dated tree implies simultaneous diversification (a 'hard' polytomy) rather than phylogenetic uncertainty, and can result in misleading inferences regarding divergence times (M.S.Y. Lee, pers. comm., 2021). We therefore also calculated a consensus that retained clades if they were present in less than 50% of the post-burnin trees provided that they were compatible with the 50% majority rule consensus topology (using the 'contype=allcompat' command in MrBayes). A BPP <0.5 (which applies to those clades present in the 'allcompat' consensus but not the 50% majority rule consensus) was considered very weak support. Selected estimates of divergence times in the tip-dating analysis are given in Table 4.

2.3. Identification of unstable taxa using Rogue

We used the R package Rogue v. 2.1.0 (Smith, 2022) to objectively identify unstable taxa from all our analyses, based on the most parsimonious trees from each MP analysis, and the post-burnin trees from each Bayesian analysis. In each case, we used the 'splitwise phylogenetic information content' criterion recommended by Smith (2021) to identify the most unstable taxa. For our MP analyses, we specified a threshold of 100, corresponding to the strict consensus, whereas for our Bayesian analyses we specified a threshold of 50, corresponding to the 50% majority rule consensus, reflecting the different types of consensuses we used to summarize the trees from these analyses. We then pruned the unstable taxa identified by Rogue using the 'drop.tip' function in the R package ape v. 5.6 (Paradis and Schliep, 2019). The pruned most parsimonious trees from the MP analyses were then summarized in TNT, again using strict consensus, and the pruned post-burnin trees from the Bayesian analyses were summarized in MrBayes, again using 50% majority rule consensus, except for the tip-dating analysis, for which we used the 'allcompat' majority rule consensus (see above). The trees from all our analyses (both before and after pruning of unstable taxa identified by Rogue) can be found in SOM.

3. Results

3.1. Undated Bayesian analysis of the molecular dataset

Undated Bayesian analysis of the molecular dataset results in a fully resolved 50% majority rule consensus, with BPPs of 1.00 for most nodes (Fig. 1), indicating the presence of strong phylogenetic signal. This is confirmed by the fact that no taxa were identified as unstable by Rogue (Table 3).

<FIGURE 1 ABOUT HERE>

Within Platyrrhini, Pitheciidae (including the Greater Antillean subfossil *Xenothrix*) is sister to the remaining families, and Aotidae, Cebidae, and Callitrichidae form a clade to the exclusion of Atelidae. In terms of interfamilial relationships, only the branching relationship between Aotidae (=*Aotus*), Cebidae, and Callitrichidae is not robustly resolved, with weak support (BPP = 0.53) for Aotidae as sister to Callitrichidae. All intrafamilial relationships are also strongly supported, except that *Ateles* + *Brachyteles* receives only moderate support (BPP = 0.83); there is thus strong support for a sister relationship between *Callicebus* and *Xenothrix*, and for monophyly of the subfamilies Atelinae (= *Ateles* + *Brachyteles* + *Lagothrix*) and Pitheciinae (= *Cacajao* + *Chiropotes* + *Pithecia*).

3.2. Maximum parsimony and undated Bayesian analysis of the morphological dataset

In contrast to the molecular analysis, analysis of the morphological dataset using both MP and undated Bayesian analysis results in much less well-resolved topologies. The MP topology (strict consensus of four shortest trees, each of 1829 steps; Fig. 2) is more resolved than the Bayesian topology (Fig. 3A), but this additional resolution is mainly due to the presence of clades that are weakly supported, as indicated by bootstrap values <50% (see Brown et al., 2017; O'Reilly et al., 2018). The MP topology places *Parvimico* sister to *Catopithecus* within Catarrhini, and *Perupithecus* sister to all other platyrrhines, whereas the Bayesian analysis places both these taxa in a polytomy at the base of crown Anthropoidea. Both analyses place *Branisella* as sister to the remaining platyrrhines, which comprise a single, largely unresolved clade in the Bayesian analysis, but in the MP analysis there is additional resolution, with the fossil taxa

Dolichocebus, *Mazzonicebus* + *Soriacebus* + *Canaanimico*, and *Homunculus* + *Carlocebus* forming successively closer sister taxa to a clade that includes all the modern genera. Relationships between the modern families are not resolved in either analysis, but both recover monophyly of crown Atelidae, crown Pitheciinae, crown Callitrichidae, crown Callitrichidae + *Lagonimico*, *Cebus* + *Acrecebus*, '*Aotus*' *dindensis* + *Mohanamico*, and *Saimiri* + *Neosaimiri*; most of these clades receive moderate or strong support in the Bayesian analysis, but not in the MP analysis, in which only four platyrrhine clades (*Homunculus* + *Carlocebus*, *Callithrix* + *Cebuella*, *Cacajao* + *Chiropotes*, and *Cacajao* + *Chiropotes* + *Pithecia*) receive bootstrap support of >50%.

Despite the lack of resolution in the strict consensus, no taxa were identified as unstable by Rogue in the MP analysis of the morphological dataset. By contrast, Rogue identified seven taxa as unstable in the equivalent Bayesian analysis (Table 3); six of these are fossil taxa that are amongst the most incomplete in the morphological dataset, but the second most unstable taxon, the subfossil *Xenothrix*, is scored for nearly half of the morphological characters (Table 3), suggesting that conflicting phylogenetic signals are the cause of its instability, rather than lack of information.

<FIGURE 2 ABOUT HERE>

<FIGURE 3 ABOUT HERE>

<TABLE 3 ABOUT HERE>

After a posteriori pruning of these seven unstable taxa, the 50% majority rule consensus from the Bayesian analysis is (as expected) better resolved, and clades that were already present

before pruning now receive higher support (Fig. 3B). There is now a distinct, strongly supported crown platyrrhine clade that is sister to a moderately supported clade that comprises the fossil taxa *Dolichocebus*, *Mazzonicebus* + *Soriacebus*+*Canaanimico*, and *Homunculus* + *Carlocebus*. Within crown Platyrrhini, there is now some interfamilial resolution, but this shows several areas of conflict with the molecular topology (Fig. 1). Most obviously, Pitheciinae (including *Cebupithecia* and *Nuciruptor* as stem taxa) is in a weakly supported clade with Atelidae and *Cebus* + *Acrecebus*, and hence neither Pitheciidae nor Cebidae are monophyletic. Comparing the Bayesian analysis after deletion of the seven rogue taxa with the MP analysis, there are a few topological differences worth noting: the MP analysis placed *Panamacebus* in a clade with crown Callitrichidae, *Lagonimico*, '*Aotus*' *dindensis*, and *Mohanamico*, whereas *Panamacebus* was unstable in the Bayesian analysis; the Bayesian analysis strongly supported *Antillothrix* + *Paralouatta*, whereas the relationship between these two taxa was unresolved in the MP analysis; and the Bayesian analysis placed the fossil *Dolichocebus*, *Mazzonicebus* + *Soriacebus* + *Canaanimico*, and *Homunculus* + *Carlocebus* in a clade, sister to crown Platyrrhini, whereas these fossil taxa were paraphyletic with respect to crown platyrrhines in the MP analysis.

3.3. Molecular scaffold analysis of the morphological dataset using maximum parsimony and Bayesian inference

Maximum parsimony analysis of the morphological dataset with the constraint of Kay et al. (2019) enforced as a molecular scaffold recovered three shortest trees (length = 1877 steps), resulting in a nearly fully resolved strict consensus (Fig. 4A); the sole lack of resolution concerns the position of *Cebupithecia*. However, the equivalent Bayesian analysis results in a highly unresolved 50% majority rule consensus (Fig. 5A), with a large polytomy that includes all our

platyrrhine taxa except *Branisella*. Perhaps unsurprisingly, only one taxon is identified as unstable by Rogue in the MP molecular scaffold analysis (*Cebupithecia*), whereas five were found to be unstable for the equivalent Bayesian analysis (Table 3).

<FIGURE 4 ABOUT HERE>

<FIGURE 5 ABOUT HERE>

After deletion of these unstable taxa, the MP (Fig. 4B) and Bayesian (Fig. 5B) molecular scaffold topologies are largely similar. For example, both analyses agree in placing *Stirtonia* sister to *Alouatta*, within crown Atelidae; *Neosaimiri* and *Panamacebus* within crown Cebidae, in a clade with *Saimiri* to the exclusion of *Cebus*; and *Lagonimico* and '*Aotus*' *dindensis* + *Mohanamico* as successive sister taxa to crown Callitrichidae; *Nuciruptor* as a stem pitheciine; and *Dolichocebus*, *Mazzonicebus* + *Soriacebus* + *Canaanimico*, and *Homunculus* + *Carlocebus* all fall outside crown Platyrrhini.

However, there are a few notable differences between the MP and Bayesian analyses despite the use of an identical molecular scaffold. For example, the MP analysis placed *Parvimico* sister to *Catopithecus* (as in the unconstrained MP analysis), whereas the Bayesian analysis found *Parvimico* to be unstable (as in the unconstrained Bayesian analysis). In the Bayesian analysis *Xenothrix*, *Antillothrix*, and *Paralouatta* collectively formed a Greater Antillean clade, sister to *Callicebus* (note that *Xenothrix* was constrained to form a clade with *Callicebus* in the molecular scaffold, following Woods et al., 2019). By contrast, in the MP analysis, *Antillothrix* + *Paralouatta* was sister to Atelidae. In the MP analysis, *Proteropithecia* formed a clade with *Mazzonicebus*, *Soriacebus*, and *Canaanimico*, *Tremacebus* was sister to

Aotidae + Cebidae + Callitrichidae within crown Platyrrhini, and *Acrecebus* was sister to *Callicebus*, whereas in the Bayesian analysis *Proteropithecia*, *Tremacebus*, and *Acrecebus* were all unstable. The MP analysis found *Cebupithecia* to be unstable, whereas the Bayesian analysis placed *Cebupithecia* as a stem pitheciine, sister to *Nuciruptor*. Perhaps most striking, the MP analysis placed *Perupithecus* within crown Callitrichidae, sister to *Leontopithecus*, whereas *Perupithecus* was unstable in the Bayesian analysis.

3.4. Bayesian undated total evidence analysis

Bayesian undated analysis of the total evidence dataset results in a relatively unresolved 50% majority rule consensus (Fig. 6A), with a large polytomy comprising all of the American taxa, except *Parvimico*, which was placed deeper within the tree. Given the very strong, consistent phylogenetic signal present in the molecular data (Fig. 1), and the relatively weak/conflicting morphological signal (Figs. 2 and 3), this lack of resolution is almost certainly due to instability in the relationships of the fossil and subfossil taxa, which are represented by morphological data only (with the exception of *Xenothrix*).

<FIGURE 6 ABOUT HERE>

Only a few relationships received moderate or strong support, namely crown Atelidae and all relationships within that clade (including the fossil *Stirtonia* as sister to *Alouatta*), crown Pitheciidae, *Callithrix* + *Cebuella*, *Callithrix* + *Cebuella* + *Callimico*, '*Aotus*' *dindensis* + *Mohanamico*, *Soriacebus* + *Canaanimico*, and *Homunculus* + *Carlocebus*. Interestingly, *Perupithecus* was placed with crown callitrichids, although this relationship was weakly

supported. Indeed, Rogue identified *Perupithecus* as unstable, together with five other taxa, all fossil and all highly incomplete: *Parvimico*, *Chilecebus*, *Acrecebus*, *Tremacebus*, and *Panamacebus* (Table 3). The 50% majority rule consensus that results after pruning of these unstable taxa is shown in Figure 6B: a number of other clades now receive moderate to strong support, including *Aotus* + Callitrichidae + Cebidae, Callitrichidae (including the stem taxon *Lagonimico*), crown Callitrichidae (i.e., excluding *Lagonimico*), Cebidae, and *Saimiri* + *Neosaimiri*. Other relationships that still receive only weak support, but are nevertheless worth noting, include *Nuciruptor* and *Cebupithecia* as stem pitheciines, a Greater Antillean clade comprising subfossil taxa *Xenothrix*, *Antillothrix*, and *Paralouatta*, with *Callicebus* sister to this, and *Proteropithecia* in a clade with *Mazzonicebus*, *Soriacebus*, and *Canaanimico*. Even after pruning of unstable taxa, the 50% majority consensus does not recover a clearly distinct crown platyrrhine clade; instead, there is a large polytomy that includes all platyrrhines except *Branisella*.

3.5. Bayesian tip-dating total evidence analysis

Tip-dating Bayesian analysis of the total evidence dataset likewise resulted in a largely unresolved 50% majority rule consensus (Fig. 7A), again probably due to the destabilizing effects of including fossil taxa (note that both phylogenies shown in Figure 7 are more resolved 'allcompat' consensus trees, to allow easier interpretation of divergence dates; branches that are collapsed in the 50% majority rule consensus are indicated with dotted lines). There is a large polytomy comprising all of the American taxa, except *Parvimico* and *Perupithecus*, which branched deeper within the tree

<FIGURE 7 ABOUT HERE>

Several of the clades that receive moderate or strong support (BPP ≥ 0.75) in the undated total evidence analysis receive similar support in the tip-dating analysis, including Atelidae and all relationships within that clade (once again with *Stirtonia* sister to *Alouatta*), crown Pitheciidae, '*Aotus*' *dindensis* + *Mohanamico*, and *Homunculus* + *Carlocebus*. However, some clades that are not strongly supported in the undated analysis receive moderate to strong support in the tip-dating analysis, including a clade comprising the fossil taxa *Cebupithecia*, *Nuciruptor* and extant pitheciines, a clade comprising the fossil *Lagonimico* and extant callitrichids, *Saimiri* as sister to *Neosaimiri*, and *Antillothrix* sister to *Paralouatta*. In contrast to the undated analysis, in which *Perupithecus* was placed with crown callitrichids, the dated analysis placed *Perupithecus* as a basal stem platyrrhine, with only *Parvimico* found to branch deeper.

Six taxa were again identified as unstable by Rogue, of which four were fossil taxa that were also unstable in the undated analysis: *Perupithecus*, *Chilecebus*, *Acrecebus*, and *Tremacebus*. However, *Parvimico* and *Panamacebus* were not found to be unstable in the dated analysis, whereas two different taxa—the fossil *Proteropithecia* and the extant *Aotus*—were. As expected, the 50% majority rule consensus is once again better resolved after pruning these unstable taxa (Fig. 7B). *Parvimico* is now weakly supported as the earliest diverging member of Platyrrhini (note that the older *Perupithecus* was pruned as unstable), and there is now weak support for a clade comprising the Early Miocene taxa *Mazzonicebus*, *Soriacebus*, *Canaanimico*, *Dolichocebus*, *Homunculus*, and *Carlocebus*. There is now also moderate support for a distinct crown platyrrhine clade that excludes all the pre-Laventan (Middle Miocene) taxa. Within this crown clade, there is a basal trichotomy comprising Atelidae, Pitheciidae, and Cebidae +

Callitrichidae (note that *Aotus* has been pruned as an unstable taxon, and so is no longer present). Interestingly, *Panamacebus* (which was described as a cebid by Bloch et al., 2016, and which was unstable in the undated analysis) is placed outside crown Platyrrhini, and is weakly supported as its sister taxon.

Focusing now on divergence times (see Table 4), the oldest split within total-clade Platyrrhini found here is between the Early Miocene fossil *Parvimico* and the remaining taxa, with a median estimated age of 34.0 Ma and 95% highest posterior density (HPD) of 31.8–36.2 Ma. The age of crown Platyrrhini is dated to the late Oligocene or Early Miocene (median estimate = 24.0 Ma; 95% HPD = 20.8–27.0 Ma). The divergence between *Callicebus* and the Greater Antillean clade is dated to the Early-to-Middle Miocene (median estimate = 16.8 Ma; 95% HPD = 12.0–21.4 Ma). The first divergence within the Greater Antillean clade itself (the split between *Xenothrix* and *Antillothrix* + *Paralouatta*) has important biogeographical implications, as it provides a potential minimum age for dispersal from the mainland; however, this divergence is only weakly constrained to some point from the Middle Miocene to the Pliocene here (median estimate = 9.3 Ma; 95% HPD = 3.4–16.1 Ma). Selected estimated divergence times are summarized in Table 4. Among the fossil taxa, the very short temporal branch (0.02 Ma) leading to *Stirtonia* in both analyses is congruent with its being ancestral to the extant *Alouatta*, but there are no other plausible ancestor-descendant relationships among our fossil taxa.

<TABLE 4 ABOUT HERE>

4. Discussion

Our unconstrained analyses of the Kay et al. (2019) morphological matrix, using both MP and Bayesian approaches, confirm that, when analyzed alone, this dataset fails to recover several clades within Platyrrhini that are robustly supported by molecular data; these clades include the families Cebidae and Pitheciidae, and also Callitrichidae + Cebidae + Aotidae, which is a feature of all recent molecular phylogenies of Platyrrhini. Kay et al. (2008) and Bloch et al. (2016) found similar results with unconstrained MP analyses of earlier versions of this dataset. For this reason, most recent phylogenetic analyses of platyrrhine relationships using morphological data have employed a molecular scaffold (Kay, 2015; Bloch et al., 2016; Marivaux et al., 2016a; Kay et al., 2019).

However, we note here that our MP molecular scaffold analysis recovered positions for several fossil taxa that appear anomalous. *Acrecebus* was described as a cebid by Kay and Cozzuol (2006), and has been consistently recovered within Cebidae in previous phylogenetic analyses (Kay, 2015; Bloch et al., 2016; Marivaux et al., 2016a; Kay et al., 2019), but our MP molecular scaffold analysis placed it as sister to *Callicebus*. *Perupithecus* is the oldest American taxon included in our taxon set, and has been placed outside crown Platyrrhini in previous phylogenetic analyses (Bond et al., 2015; Kay et al., 2019), but our MP molecular scaffold placed it sister to the extant callitrichid *Leontopithecus*. Finally, *Cebupithecia* shares numerous distinctive apomorphies with living pitheciines (Kay et al., 2013; Rosenberger, 2020), and it has been consistently identified as pitheciine in recent phylogenetic analyses (Kay, 2015; Bloch et al., 2016; Marivaux et al., 2016a; Kay et al., 2019; Ni et al., 2019), but it was found to be unstable (although still within a clade that also includes living pitheciids, the fossil pitheciine *Nuciruptor*, and the Greater Antillean subfossil *Xenothrix*) in our MP molecular scaffold analysis.

These results may be due, at least in part, to the fact that we did not scale the weights of the ordered characters in the morphological matrix, and we also treated polymorphisms (3.6% of the total character scores; see Methods) as missing data; in both cases, this was to ensure comparability with our Bayesian analyses because MrBayes v. 3.2.7a does not allow character scaling, and always treats polymorphisms as missing data. This is unlike most previous molecular scaffold analyses that have used versions of this dataset (Kay, 2015; Bloch et al., 2016; Marivaux et al., 2016a; Kay et al., 2019). However, we note that the equivalent Bayesian analysis did not support these anomalous relationships: *Acrecebus* and *Perupithecus* were both found to be unstable and *Cebupithecia* was placed as a stem pitheciine as expected.

There is an ongoing debate as to whether MP or model-based approaches, either with or without the incorporation of temporal information via tip dating, are more appropriate for analyzing morphological data, and whether currently used models of discrete morphological character evolution (the Markov or Mk model of Lewis, 2001, and variants) are biologically realistic (e.g., Goloboff and Pol, 2005; Huelsenbeck et al., 2011; Lee and Worthy, 2012; Xu and Pol, 2013; Simmons, 2014; Wright and Hillis, 2014; Goloboff et al., 2018a, 2018b, 2019; Turner et al., 2017; O'Reilly et al., 2016, 2018a, 2018b; King, 2019, 2021; Puttick et al., 2019; Smith, 2019; Mongiardino Koch et al., 2021; Pugh, 2022). Although our study considered only a single morphological dataset, we note that, with a molecular scaffold enforced, Bayesian analysis appeared to recover relationships that are overall in better agreement with other recent published studies regarding the affinities of fossil platyrrhines than did the equivalent MP analysis. This is in contrast to Pugh's (2022) recent study of the phylogeny of Miocene hominoids, which found that MP resulted in topologies that appeared more plausible (based on current evidence) than did Bayesian analysis, including when a molecular scaffold was enforced. Pugh (2022:11–14)

discussed possible reasons for the differences between the two methods, and we agree that this issue requires further investigation, considering multiple morphological datasets. Regardless, we consider total evidence analysis (where feasible) to be preferable to molecular scaffold analysis, for the reasons outlined in our Introduction, and so we focus on previous total evidence analyses of Platyrrhini and our own total evidence results for the remainder of this section. We nevertheless note that the relationships of several fossil taxa are the same between our molecular scaffold and total evidence analyses, namely *Lagonimico*, *Mohanamico* and '*Aotus*' *dindensis* as stem callitrichids, *Neosaimiri* as a saimirine, *Stirtonia* as an allouatine, and *Nuciruptor* as a pitheciine.

Schrago et al. (2013) presented a total evidence analysis of Platyrrhini, and used a novel approach to infer divergence dates by first carrying out an undated total evidence analysis, and then performing a relaxed clock analysis of morphological data only on the total evidence topology, with age estimates from a separate molecular clock analysis used as node age priors. However, this approach lacks a key aspect of tip-dating, namely that the stratigraphic ages of the fossil terminals can influence their phylogenetic position (Bapst et al., 2016; Turner et al., 2017; Lee and Yates, 2018; Beck and Taglioretti, 2020; King and Beck, 2020; Beck et al., 2021; King, 2021). The morphological clock analysis of Schrago et al. (2013) also assumed a Yule prior on tree shape, which has been shown to lead, in at least some cases, to unrealistically ancient divergence dates (Condamine et al., 2015), although we note that the dates calculated by Schrago et al. (2013) in this analysis are in fact largely congruent with those presented here (Table 4). The sampling of fossil platyrrhines by Schrago et al. (2013) was also relatively restricted, and lacked a number of taxa that have been consistently associated with crown lineages, such as the *Stirtonia*, *Cebupithecia*, *Neosaimiri*, and *Lagonimico* (Kay, 2015). Indeed, only one fossil taxon

(*Proteropithecia*) fell within crown Platyrrhini (as a stem pitheciine) in the analysis of Schrago et al. (2013), and so the results of this analysis are of limited use in identifying robust fossil calibrations for divergences among crown platyrrhines. In addition, our own results raise questions about whether *Proteropithecia* is indeed a pitheciine (discussed in more detail below).

Silvestro et al. (2019) carried out a tip-dating analysis of platyrrhines that included 34 fossil taxa, using the FBD model, but the fossil taxa were not represented by character data and their relationships were constrained a priori (living taxa were represented by combined nuclear and mitochondrial sequence data only); thus, their phylogenetic position was not free to vary, and could not be informed by morphological data. Perhaps most significantly, Silvestro et al. (2019) assumed the 'Long Lineage' hypothesis, which considers that pre-Laventan platyrrhines from Patagonia are members of the crown clade (Rosenberger et al., 2009; Rosenberger, 2010, 2011, 2019; Rosenberger and Tejedor, 2013) when constraining the relationships of their fossil taxa; the 'Long Lineage' hypothesis is not supported by our analyses (see below).

Published total evidence tip-dating analyses of broad primate phylogeny, meanwhile, have typically included a relatively limited sampling of platyrrhines (e.g., Gunnell et al., 2018; Seiffert et al., 2020). An exception is that of Ni et al. (2019, their fig. S1), which included a relatively dense sampling of fossil platyrrhines as well as other primates, and which used a similar approach to that used here (specifically, the FBD tree model in combination with the IGR clock model, as implemented in MrBayes), but with a different dataset (1186 morphological characters from the dentition, cranium, postcranium and soft tissues; 658 SINE and LINE insertion characters) that was focused on relationships within Haplorhini as a whole. However, of the 11 fossil platyrrhines included by Ni et al. (2019), only two fell within crown Platyrrhini in their analysis: '*Aotus*' *dindensis* as sister to the extant *Aotus azarae*, and *Mohanamico*

hershkovitzi as a stem callitrichid. Several other recent analyses (Kay, 2015; Bloch et al., 2016; Marivaux et al., 2016a; Kay et al., 2019) have failed to support '*A.*' *dindensis* as an aotid, and Kay (2015) suggested that it may in fact be the same taxon as *M. hershkovitzi*. These recent analyses have also placed two fossil taxa that Ni et al. (2019) found to be stem platyrrhines—namely *Stirtonia* and *Neosaimiri*—within crown Platyrrhini (Kay, 2015; Bloch et al., 2016; Marivaux et al., 2016a; Kay et al., 2019). Like Schrago et al. (2013), Ni et al. (2019) did not include several other fossil taxa that have been suggested to fall within crown Platyrrhini, namely *Proteropithecia*, *Nuciruptor*, and *Lagonimico* (Kay, 2015). We also note that Ni et al. (2019) incorrectly assigned an age of 0 Ma to the Miocene *Cebupithecia*, which may have influenced their results.

The analyses we present here should therefore be of interest because they are the first to include a diverse sampling of fossil platyrrhines, including putative members of many crown lineages, in a true total evidence approach. As such, they should help identify robust calibrations within crown Platyrrhini for use in molecular clock analyses, as well as provide their own estimates of platyrrhine relationships and divergence times.

Focusing first on the living taxa, relationships among extant taxa within the families Callitrichidae, Atelidae and Pitheciidae recovered in our total evidence analyses are congruent with recent molecular analyses (Perelman et al., 2011; Springer et al., 2012; Buckner et al., 2015; dos Reis et al., 2018; Garbino and Martins-Junior, 2018). However, whereas our molecular data robustly supports an interfamilial topology that agrees with other recent molecular analyses - in which Pitheciidae is the first family to diverge, and Callitrichidae, Aotidae and Cebidae form a clade to the exclusion of Atelidae (Perelman et al., 2011; Springer et al., 2012; dos Reis et al.,

2018) -, relationships between the extant families are weakly supported in our undated and tip-dating total evidence analyses, even after deleting unstable taxa.

In terms of relationships among our non-living taxa, perhaps the most significant aspect of both analyses is the fact that all American primate taxa older than the Laventan (Middle Miocene) present in our analyses fall outside crown Platyrrhini. Of particular interest are the positions of *Panamacebus* and *Proteropithecia*. The Early Miocene (21.1–18.748 Ma) *Panamacebus* was originally described as a cebid by Bloch et al. (2016), and has been recovered within crown Cebidae in several published phylogenetic analyses that have used a molecular scaffold approach (Bloch et al., 2016; Marivaux et al., 2016a; Kay et al., 2019). We also found *Panamacebus* to fall within crown Cebidae in our MP and Bayesian scaffold analyses. In our undated total evidence analysis, however, *Panamacebus* was found to be an unstable 'rogue' taxon, and did not form a clade with the extant cebids *Cebus* and *Saimiri*; instead, it was part of a large polytomy. In our tip-dating analysis, meanwhile, *Panamacebus* was placed as sister to (rather than within) crown Platyrrhini after deleting unstable taxa, and there was moderate support (BPP = 0.76) for this crown platyrrhine clade that excludes *Panamacebus*. Thus, the additional information provided by the age of *Panamacebus* is sufficient to combine with the relatively weak morphological signal for its affinities and place it outside crown Platyrrhini in our tip-dating analysis. The results of this analysis, therefore, do not support *Panamacebus* as a cebid, or a crown-platyrrhine, in contrast to previous results; based on current evidence, we suggest that *Panamacebus* should not be used to calibrate divergences within crown Platyrrhini.

Proteropithecia is from the Collón Curá Formation of Patagonia, and its age is poorly constrained to between 19.76 and 10.4 Ma (López et al., 2019; Nivière et al., 2019; see Table 2); it may therefore in fact postdate the Laventan (which is ~13.8–11.8 Ma; Prevosti and Forasiepi,

2018). Our MP molecular scaffold and undated Bayesian total evidence analyses placed *Proteropithecia* in a clade with three late Oligocene-Early Miocene fossil taxa (*Mazzonicebus*, *Soriacebus*, and *Canaanimico*), not with extant pitheciines, whereas the equivalent tip-dating analysis (and also the morphological and Bayesian molecular scaffold analyses) found it to be an unstable taxon. This is the opposite situation to *Panamacebus*: the additional information provided by the age of *Proteropithecia* is sufficient to make its overall position more uncertain than when determined by morphological data alone. Regardless, our analyses do not support *Proteropithecia* as a fossil pitheciine. To our knowledge, the pitheciine status of *Proteropithecia* has been uncontroversial (Kay et al., 2013; Rosenberger and Tejedor, 2013; Kay, 2015; Tejedor and Novo, 2016; Rosenberger, 2020), although Kay et al. (1998a) identified some notable dental differences between *Proteropithecia* and living pitheciines in their original description of this taxon. We did not attempt a detailed reassessment of the affinities of *Proteropithecia*, but merely note that our results raise the possibility that this taxon may be a stem platyrrhine convergent on pitheciines (as has also been proposed for *Soriacebus*; Kay, 1990, 2010, 2015; Kay et al., 2013). If so, this would remove the last direct biogeographical link between the Miocene platyrrhines from Patagonia (all of which would therefore seem to be stem taxa) and crown Platyrrhini, the known fossil record of which is confined to northern South America.

Our total evidence analyses do not support the 'Long Lineage' hypothesis (Rosenberger et al., 2009; Rosenberger, 2010, 2011, 2019; Rosenberger and Tejedor, 2013), which posits that the pre-Laventan taxa are early members of crown platyrrhine lineages. This is a similar result to previous studies that have analyzed versions of the morphological matrix used here (Kay, 2015; Bloch et al., 2016; Marivaux et al., 2016a; Kay et al., 2019), except that Bloch et al. (2016), Marivaux et al. (2016) and Kay et al. (2019) all found the Early Miocene *Panamacebus* to be a

cebid, as did our MP and Bayesian molecular scaffold analyses. By contrast, our total evidence analyses do not support any fossil taxon older than the Middle Miocene as a crown platyrrhine, with the oldest crown forms (the crown atelid *Stirtonia* and the stem callitrichid *Lagonimico*) having a maximum age of 13.608 Ma (Table 2). However, our estimated age for crown Platyrrhini (median date = 24.0 Ma; 95% HPD = 20.8-27.0 Ma) suggests that crown platyrrhines should be present in the Early Miocene and possibly late Oligocene. Given the position of Miocene platyrrhines from Patagonia as stem taxa, it seems likely that continuing fieldwork in Amazonia (Marivaux et al., 2016a, 2016b, 2020a; Kay et al., 2019; Seiffert et al., 2020; Antoine et al., 2021) and elsewhere in northern South America will have the greatest chance of finding fossil evidence of the earliest stages of the crown platyrrhine radiation.

Another notable aspect of both of our undated and tip-dating total evidence analyses is recovery of a clade comprising the three Greater Antillean subfossil taxa *Xenothrix*, *Antillothrix*, and *Paralouatta*, which is sister to *Callicebus*. This clade was also found by Marivaux et al. (2016a), but not by Kay (2015) or Kay et al. (2019), even though we used the latter's morphological matrix here; however, all of these previous studies were based on parsimony analysis of a morphological matrix with a molecular scaffold enforced, which precludes synergistic interactions between morphological and molecular data and which does not take into account temporal information. Indeed, our own MP molecular scaffold analysis also did not recover a Greater Antillean clade, although our Bayesian molecular scaffold analysis did. The Greater Antillean clade received only weak support in our total evidence analyses, even after a posteriori pruning of unstable taxa. Nevertheless, it is of interest because it implies that the presence of these genera in the Greater Antilles may be the result of a single dispersal event. It is worth noting that recent molecular studies have found that the Greater Antillean radiations of

solenodonotan ‘insectivores’ (Brace et al., 2016; Buckley et al., 2020) and caviomorph rodents (Woods et al., 2018) appear to be the result of single dispersal events.

However, of the three Greater Antillean taxa, DNA sequence data are currently only available for *Xenothrix* (Woods et al., 2018); molecular data (e.g., ancient DNA or protein sequences) from *Antillothrix*, *Paralouatta*, and also *Insulacebus* (not included here; Cooke et al., 2011), will be needed to rigorously test monophyly of the Greater Antillean clade. In addition, we included only a single extant callicebine (*Callicebus*), whereas Woods et al. (2018) included multiple representatives of all three extant callicebine genera (*Callicebus*, *Cheracebus*, and *Plecturocebus*), and found *Xenothrix* to be sister to *Cheracebus*; addition of *Cheracebus* and *Plecturocebus* to the matrix used here would allow further testing of this hypothesis. We note, however, that the divergence dates presented here are still congruent with monophyly of the Greater Antillean clade when combined with those of Woods et al. (2018): specifically, Woods et al. (2018) estimated that *Xenothrix* diverged from *Cheracebus* 10.8 Ma (95% HPD = 5.2–14.9 Ma), and we estimate the age of the common ancestor of the Greater Antillean taxa to be younger than this (median date = 9.3 Ma; 95% HPD = 3.4–16.1 Ma).

Finally, we note that MacPhee et al. (2003) described an isolated platyrrhine astragalus from the Domo de Zaza locality in Cuba, that they considered to be closely related to the Cuban subfossil *Paralouatta varonai* and which they named *Paralouatta marianae*. MacPhee et al. (2003) concluded that Domo de Zaza is most likely Early Miocene (Burdigalian, 20.44–15.97 Ma; Cohen et al., 2013; updated), although radiometric dating with strontium isotopes was inconclusive. If a Burdigalian age for *P. marianae* is correct, then it suggests that our estimated age for the Greater Antillean clade is too young (if *P. varanaoi* and *P. marianae* are indeed

closely related), or it indicates at least one other dispersal event by platyrrhines to the Greater Antilles.

Based on the results of our molecular scaffold and total evidence analyses, the following four South American fossil primate taxa can be identified as representing robust calibrations for informing the minimum bound on divergences within Platyrrhini: *Stirtonia*, which is strongly supported as a stem alouattine, and so provides a minimum bound on age of the Alouattinae-Atelinae split of 13.363 Ma; *Neosaimiri*, which is strongly supported as a stem saimirine, and so provides a minimum bound on the age of the Cebinae-Saimirinae split of 12.272 Ma; *Cebupithecia*, which is strongly supported as a pitheciine, and so provides a minimum bound on the age of Pitheciinae-Callicebinae split of 13.032 Ma; and *Lagonimico*, which is strongly supported as a stem callitrichid, and so provides a minimum bound on the divergence of Callitrichidae from its sister family (which varies depending on the precise relationship of Aotidae to Callitrichidae and Cebidae) of 13.183 Ma. We note here, however, that the tip-dating total evidence analysis of Ni et al. (2019) suggests a very different set of relationships, with *Stirtonia* and *Neosaimiri* both placed outside crown Platyrrhini (*Cebupithecia* and *Lagonimico* were not included in Ni et al.'s, 2019 analysis).

Studies suggest that accurate estimates of divergence times under the FBD model require dense sampling of fossil taxa (Klopfstein et al., 2019; O'Reilly and Donoghue, 2019). The morphological dataset we used here, namely that of Kay et al. (2019), includes most named South American primate genera (note that *Szalatavus*, *Killikaike*, and *Laventiana* have been argued to be synonyms of *Branisella*, *Homunculus*, and *Neosaimiri* respectively; Kay, 2015), but this is a reflection of the overall paucity of the known fossil record (although this continues to improve thanks to ongoing, extensive efforts by a number of different research teams; Marivaux

et al., 2016a, 2016b, 2020a; Novo et al., 2017, 2021; Kay et al., 2019; Seiffert et al., 2020; Antoine et al., 2021). However, this dataset includes a limited selection of fossil catarrhines and stem anthropoids, some of which (e.g., *Talahpithecus*, *Proteopithecus*, and oligopithecids) may be of particular relevance for understanding the origin of platyrrhines, including the timing of their arrival in South America (Bond et al., 2015). For this reason, the divergence times estimated in our total evidence tip-dating analyses should be treated with caution. Nevertheless, our tip-dating analysis suggests that platyrrhines arrived in South America between after 37.1 Ma and before 31.8 Ma, based on the maximum estimate for the Platyrrhini-Catarrhini split (95% HPD: 37.1–33.9 Ma) and the minimum estimate for the divergence of the earliest diverging stem platyrrhine in our dataset, *Parvimico* (95% HPD: 36.2–31.8 Ma; note that *Perupithecus* was found to be unstable). Notably, this is very similar to Seiffert et al.'s (2020) estimate for the timing of dispersal of a second South American primate taxon, the parapithecid *Ucayalipithecus*, namely 35.1–31.7 Ma, which these authors noted coincides with a major drop in global sea levels (Miller et al., 2008).

Our late Oligocene-Early Miocene estimate for the age of crown Platyrrhini is similar to estimates from several previous molecular clock analyses (Perelman et al., 2011; Springer et al., 2012; dos Reis et al., 2018; Woods et al., 2018; Wang et al., 2019), as well as from the novel two-stage molecular and morphological clock analysis of Schrago et al. (2013), and from the total evidence tip-dating analysis of Ni et al. (2019). It is worth noting that this is similar to the crown age of another major clade of predominantly South and Central American mammals, namely the marsupial family Didelphidae (opossums), as estimated by some molecular clock (node-dating) analyses (Jansa et al., 2014)—although others suggest a somewhat earlier age

(Steiner et al., 2005; Meredith et al., 2011; Mitchell et al., 2014; Vilela et al., 2015)—and also by total evidence tip-dating analyses (Beck and Taglioretti, 2020; Beck et al., 2021).

Node-dated molecular clock estimates for the age of crown Caviomorpha are markedly older, typically mid-to-late Eocene or earliest Oligocene (Sallam et al., 2009; Rowe et al., 2010: table 1; Meredith et al., 2011; Upham and Patterson, 2012, 2015; Voloch et al., 2013; Álvarez et al., 2017; Woods et al., 2021). Several of these studies (Voloch et al., 2013; Upham and Patterson, 2015; Álvarez et al., 2017) have calibrated the deepest divergences within crown Caviomorpha based on fossil taxa from Contamana in Peru, which have been dated to the middle Eocene (~41 Ma) and include taxa that have been referred to the caviomorph crown clade by some authors; specifically, *Eobranisamys javierpradoi* and *Eospina* sp. from Contamana were identified as early members of Cavioidea and Octodontoidea respectively by Antoine et al. (2012) and Boivin et al. (2017). However, the reported age of Contamana has been questioned (Campbell et al., 2021), and, in any case, the recent phylogenetic study of Boivin et al. (2019) suggests that all of the Contamana rodents (including *Eobranisamys* and *Eospina*) fall outside the crown Caviomorpha. Definitive crown caviomorphs have been reported from the Tinguiririca fauna of Chile (Bertrand et al., 2012), and are estimated to be 37.5–31.5 Ma based on radiometric dating (Wyss et al., 1990, 1993; Flynn et al., 2003; Bertrand et al., 2012). Given the ongoing controversy regarding the ages of Paleogene sites in Peruvian Amazonia (Campbell et al., 2021), the Tinguirirican fossils are arguably the oldest securely dated crown caviomorphs, and they indicate that crown Caviomorpha had begun to diversify by the earliest Oligocene at the latest (see also Marivaux et al., 2020b). Campbell et al. (2021, their fig. S7) presented a morphological tip-dating analysis of Caviomorpha using the matrix of Marivaux et al. (2020b; which is modified from that of Boivin et al., 2019) in which the ages of fossil taxa from localities

that they considered to be of controversial age (at Santa Rosa, Shapaja, and Contamana; Campbell et al., 2021) were allowed to vary between 56 and 0 Ma. In this analysis, the median estimate for the age of crown Caviomorpha was 40.2 Ma, with a 95% HPD of 43.5–37.5 Ma. Collectively, then, current evidence suggests that crown Caviomorpha is at least 10 million years older than crown Platyrrhini.

The tip-dating analysis of Campbell et al. (2021) suggests that the dispersal of Caviomorpha to South America occurred after 44.5 Ma but before 37.5 Ma. This is close to, but does not overlap with, our composite estimate for the timing of dispersal of platyrrhines (37.2–30.9 Ma), or Seiffert et al.'s (2020) estimate for the dispersal of the parapithecid lineage represented by *Ucayalipithecus* (35.1–31.7 Ma). However, the accuracy of divergence dates estimated by tip-dating approaches needs further exploration (Beck and Lee, 2014; Drummond and Stadler, 2016; Puttick et al., 2016; Ronquist et al., 2016; Parins-Fukuchi and Brown, 2017; Luo et al., 2019; King and Beck, 2020; Püschel et al., 2020; Simões et al., 2020), and some molecular clock studies have suggested that the dispersals of platyrrhines and caviomorphs could have been coincident in time (Poux et al., 2006; Loss-Oliveira et al., 2012).

As noted above, monophyly of the Greater Antillean genera *Xenothrix*, *Antillothrix*, and *Paralouatta* raises the possibility that they may be the result of a single dispersal event from the South American mainland; if so, our divergence estimates permit a wide range of ages for this event, spanning from the earliest Miocene to the Late Pliocene (21.4–3.4 Ma). Although poorly constrained, this nevertheless overlaps with the inferred timing of dispersal of caviomorph rodents to Caribbean landmasses based on the molecular clock (node-dating) analysis of Woods et al. (2021), which is 21.7–7.1 Ma. These estimates are therefore permissive of synchronous dispersals by platyrrhines and caviomorphs from mainland South America to the Greater

Antilles. However, the presence of a platyrrhine (*Paralouatta marianae*) in the Early Miocene of Cuba (MacPhee et al., 2003) discussed above, and also chinchilloid caviomorphs (*Borikenomys praecursor* and a second, indeterminate taxon) in the early Oligocene of Puerto Rico (Marivaux et al., 2020b), suggest that there have in fact been multiple dispersals by both platyrrhines and caviomorphs, and hence a complex biogeographic history for the Greater Antillean members of these clades.

5. Conclusions

The results presented here provide a new perspective on our current understanding of platyrrhine phylogeny. Specifically, our use of total evidence analysis, together with a formal information theoretic approach for identifying unstable taxa, has helped clarify which fossil taxa can be robustly placed within specific platyrrhine clades, and which are of more uncertain affinities. By contrast, molecular scaffold analysis using MP (but not Bayesian inference) resulted in a number of anomalous relationships. The differences between our undated and tip-dating total evidence analyses also reveal the impact that temporal information can have on phylogenetic inference, and we recommend that, where feasible, researchers explore both approaches, particularly as tip dating allows for the inference of divergence times between taxa. Total evidence analysis represents a powerful and flexible (albeit computationally more intensive) alternative phylogenetic approach to molecular scaffold analysis, and it will undoubtedly become more widely used in phylogenetic analyses of primate clades that include both extant and fossil representatives, particularly as the methods and models used to implement it become more sophisticated and biologically realistic.

Acknowledgments

We thank Pierre-Olivier Antoine, Laurent Marivaux, and Mike Lee for discussion. Laurent Marivaux, Rich Kay, and one anonymous reviewer provided detailed and constructive reviews, and the Associate Editor Yaowalak Chaimanee and the Co-Editor-in-Chief Andrea Taylor provided additional feedback and advice, all of which enabled us to greatly improve this paper. This work used JASMIN, the UK's collaborative data analysis environment (https://jasmin.ac.uk). Funding for this paper was provided by NERC Standard Grant 'Rise of the continent of the monkeys (NE/T000341/1).

References

Alfaro, M.E., Zoller, S., Lutzoni, F., 2003. Bayes or bootstrap? A simulation study comparing the performance of Bayesian Markov chain Monte Carlo sampling and bootstrapping in assessing phylogenetic confidence. Mol. Biol. Evol. 20, 255-266.

Álvarez, A., Arévalo, R.L.M., Verzi, D.H., 2017. Diversification patterns and size evolution in caviomorph rodents. Biol. J. Linn. Soc. 121, 907–922.

Anderson, V.J., Horton, B.K., Saylor, J.E., Mora, A., Tesón, E., Breecker, D.O., Ketcham, R.A., 2016. Andean topographic growth and basement uplift in southern Colombia: Implications for the evolution of the Magdalena, Orinoco, and Amazon river systems. Geosphere 12, 1235–1256.

Antoine, P.-O., Marivaux, L., Croft, D.A., Billet, G., Ganerød, M., Jaramillo, C., Martin, T., Orliac, M.J., Tejada, J., Altamirano, A.J., Duranthon, F., Fanjat, G., Rousse, S., Gismondi, R.S., 2012. Middle Eocene rodents from Peruvian Amazonia reveal the pattern and timing of caviomorph origins and biogeography. Proc. R. Soc. B Biol. Sci. 279, 1319–1326.

Antoine, P.-O., Yans, J., Castillo, A.A., Stutz, N., Abello, M.A., Adnet, S., Custódio, M.A.,

Benites-Palomino, A., Billet, G., Boivin, M., Herrera, F., Jaramillo, C., Mártinez, C., Moreno, F., Navarrete, R.E., Negri, F.R., Parra, F., Pujos, F., Rage, J.-C., Ribeiro, A.M., Robinet, C., Roddaz, M., Tejada-Lara, J.V., Varas-Malca, R., Ventura Santos, R., Salas-Gismondi, R., Marivaux, L., 2021. Biotic community and landscape changes around the Eocene–Oligocene transition at Shapaja, Peruvian Amazonia: Regional or global drivers? Glob. Planet. Change 202, 103512.

Asher, R.J., Emry, R.J., McKenna, M.C., 2005. New material of Centetodon (Mammalia, Lipotyphla) and the importance of (missing) DNA sequences in systematic paleontology. J. Vertebr. Paleontol. 25, 911-923.

Bapst, D.W., Wright, A.M., Matzke, N.J., Lloyd, G.T., 2016. Topology, divergence dates, and macroevolutionary inferences vary between different tip-dating approaches applied to fossil theropods (Dinosauria). Biol. Lett. 12, 20160237.

Barba-Montoya, J., Tao, Q., Kumar, S., 2021. Molecular and morphological clocks for estimating evolutionary divergence times. BMC Ecol. Evol. 21, 83.

Beck, R.M.D., Lee, M.S.Y., 2014. Ancient dates or accelerated rates? Morphological clocks and the antiquity of placental mammals. Proc. R. Soc. B Biol. Sci. 281, 20141278.

Beck, R.M.D., Taglioretti, M.L., 2020. A nearly complete juvenile skull of the marsupial *Sparassocynus derivatus* from the Pliocene of Argentina, the affinities of “sparassocynids”, and the diversification of opossums (Marsupialia; Didelphimorphia; Didelphidae). J. Mammal. Evol. 27, 385–417.

Beck, R.M.D., Voss, R., Jansa, S., 2022. Craniodental morphology and phylogeny of marsupials. Bull. Am. Mus. Nat. Hist. 457, 1-350.

Benton, M.J., Donoghue, P.C.J., Asher, R.J., Friedman, M., Near, T.J., Vinther, J., 2015.

Constraints on the timescale of animal evolutionary history. Palaeontol. Electron. 18, 1–106.

Bertrand, O.C., Flynn, J.J., Croft, D.A., Wyss, A.R., 2012. Two new taxa (Caviomorpha, Rodentia) from the early Oligocene Tinguiririca Fauna (Chile). Am. Mus. Novit. 2012, 1–36.

Bloch, J.I., Woodruff, E.D., Wood, A.R., Rincon, A.F., Harrington, A.R., Morgan, G.S., Foster, D.A., Montes, C., Jaramillo, C.A., Jud, N.A., Jones, D.S., MacFadden, B.J., 2016. First North American fossil monkey and early Miocene tropical biotic interchange. Nature 533, 243–246.

Boivin, M., Marivaux, L., Orliac, M.J., Pujos, F., 2017. Late middle Eocene caviomorph rodents from Contamana, Peruvian Amazonia. Palaeontol. Electron. 20.1, 19A.

Boivin, M., Marivaux, L., Antoine, P.-O., 2019. L'apport du registre paléogène d'Amazonie sur la diversification initiale des Caviomorpha (Hystricognathi, Rodentia): Implications phylogénétiques, macroévolutives et paléobiogéographiques. Geodiversitas 41, 143–245.

Bond, M., Tejedor, M.F., Campbell, K.E., Jr, Chornogubsky, L., Novo, N., Goin, F., 2015. Corrigendum: Eocene primates of South America and the African origins of New World monkeys. Nature 525, 552.

Bondesio, P., Rabassa, J., Pascual, R., Vucetich, M.G., Scillato-Yané, G.J., 1980. La formación Collon-Cura del Pilcaniyeu viejo y sus alrededores [Río Negro, República Argentina]. Su antiguedad y las condiciones ambientales según su distribución, su litogénesis sus vertebrados. Actas II Congreso Argentino de Paleontología y Bioestratigrafía y I Congreso Latinoamericano de Paleontología, Buenos Aires, pp. 85-99.

Brace, S., Thomas, J.A., Dalen, L., Burger, J., MacPhee, R.D., Barnes, I., Turvey, S.T., 2016.

Evolutionary history of the Nesophontidae, the last unplaced Recent mammal family. Mol. Biol. Evol. 33, 3095-3103.

Buckley, M., Harvey, V.L., Orihuela, J., Mychajliw, A.M., Keating, J.N., Milan, J.N.A., Lawless, C., Chamberlain, A.T., Egerton, V.M., Manning, P.L., 2020. Collagen sequence analysis reveals evolutionary history of extinct West Indies *Nesophontes* (island-shrews). Mol. Biol. Evol. 37, 2931-2943.

Buckner, J.C., Lynch Alfaro, J.W., Rylands, A.B., Alfaro, M.E., 2015. Biogeography of the marmosets and tamarins (Callitrichidae). Mol. Phylogen. Evol. 82, 413–425.

Campbell, K.E., Jr, O'Sullivan, P.B., Fleagle, J.G., de Vries, D., Seiffert, E.R., 2021. An Early Oligocene age for the oldest known monkeys and rodents of South America. Proc. Natl. Acad. Sci. USA 118, e2105956118.

Cascini, M., Mitchell, K.J., Cooper, A., Phillips, M.J., 2019. Reconstructing the evolution of giant extinct kangaroos: Comparing the utility of DNA, morphology, and total evidence. Syst. Biol. 68, 520-537.

Chen, A., White, N.D., Benson, R.B.J., Braun, M.J., Field, D.J., 2019. Total-evidence framework reveals complex morphological evolution in nightbirds (Strisores). Diversity 11, 143.

Cohen, K.M., Finney, S.C., Gibbard, P.L., Fan, J.-X., 2013; updated. The ICS international chronostratigraphic chart. Episodes 36, 199–204.

Condamine, F.L., Nagalingum, N.S., Marshall, C.R., Morlon, H., 2015. Origin and diversification of living cycads: a cautionary tale on the impact of the branching process prior in Bayesian molecular dating. BMC Evol. Biol. 15, 65.

Cooke, S.B., Rosenberger, A.L., Turvey, S., 2011. An extinct monkey from Haiti and the origins of the Greater Antillean primates. Proc. Natl. Acad. Sci. USA 108, 2699–2704.

Cooke, S.B., Mychajliw, A.M., Southon, J., MacPhee, R.D.E., 2017. The extinction of *Xenothrix mcgregori*, Jamaica's last monkey. J. Mammal. 98, 937–949.

Darlim, G., Lee, M.S.Y., Walter, J., Rabi, M., 2022. The impact of molecular data on the phylogenetic position of the putative oldest crown crocodilian and the age of the clade. Biol. Lett. 18, 20210603.

Dávalos, L.M., Velazco, P.M., Warsi, O.M., Smits, P.D., Simmons, N.B., 2014. Integrating incomplete fossils by isolating conflicting signal in saturated and non-independent morphological characters. Syst. Biol. 63, 582-600.

de Queiroz, A., Gatesy, J., 2007. The supermatrix approach to systematics. Trends Ecol. Evol. 22, 34-41.

de Vries, D., Beck, R.M.D., 2021. Total evidence tip-dating phylogeny of platyrrhine primates and 27 well-justified fossil calibrations for primate divergences. bioRxiv preprint, 2021.10.21.465342. doi.org/10.1101/2021.10.21.465342

dos Reis, M., Donoghue, P.C.J., Yang, Z., 2016. Bayesian molecular clock dating of species divergences in the genomics era. Nat. Rev. Genet. 17, 71–80.

dos Reis, M., Gunnell, G.F., Barba-Montoya, J., Wilkins, A., Yang, Z., Yoder, A.D., 2018. Using phylogenomic data to explore the effects of relaxed clocks and calibration strategies on divergence time estimation: Primates as a test case. Syst. Biol. 67, 594–615.

Drummond, A.J., Stadler, T., 2016. Bayesian phylogenetic estimation of fossil ages. Philos. Trans. R. Soc. B. Biol. Sci. 371, 20150129.

Dunn, R.E., Madden, R.H., Kohn, M.J., Schmitz, M.D., Strömberg, C.A.E., Carlini, A.A., Ré, G.H., Crowley, J., 2013. A new chronology for middle Eocene–early Miocene South American Land Mammal Ages. Geol. Soc. Am. Bull. 125, 539–555.

Edgar, R.C. 2004. MUSCLE: multiple sequence alignment with high accuracy and high throughput. Nucleic Acids Res. 32, 1792-1797.

Fleagle, J.G., Gladman, J.T., Kay, R.F., 2022. A New humerus of *Homunculus patagonicus*, a stem platyrrhine from the Santa Cruz Formation (late Early Miocene), Santa Cruz Province, Argentina. Ameghiniana 59, 78–96.

Flynn, J.J., Wyss, A.R., Charrier, R., Swisher, C.C., 1995. An Early Miocene anthropoid skull from the Chilean Andes. Nature 373, 603–607.

Flynn, J.J., Guerrero, J., Swisher, C.C., 1997. Geochronology of the Honda Group. In: Kay, R. F. Madden, R. H., Cifelli, R. L., Flynn, J. J. (Eds.), Vertebrate Paleontology in the Neotropics: The Miocene Fauna of La Venta, Colombia. Smithsonian Institution Press, Washington, D.C., pp. 44–60.

Flynn, J.J., Wyss, A.R., Croft, D.A., Charrier, R., 2003. The Tinguiririca fauna, Chile: Biochronology, paleoecology, biogeography, and a new earliest Oligocene South American land mammal "age." Palaeogeogr. Palaeoclimatol. Palaeoecol. 195, 229–259.

Garbino, G.S.T., Martins-Junior, A.M.G., 2018. Phenotypic evolution in marmoset and tamarin monkeys (Cebidae, Callitrichinae) and a revised genus-level classification. Mol. Phylogen. Evol. 118, 156–171.

Gasparini, G.M., Dutra, R.P., Perini, F.A., Croft, D.A., Cozzuol, M.A., Missagia, R.V., Lucas, S.G., 2021. On the supposed presence of Miocene Tayassuidae and Dromomerycinae (Mammalia, Cetartiodactyla) in South America. Am. Mus.Novit. 2020, 1–28.

Gatesy, J., O'Grady, P., Baker, R.H., 1999. Corroboration among data sets in simultaneous analysis: Hidden support for phylogenetic relationships among higher level artiodactyl taxa. Cladistics 15, 271-313.

Gatesy, J., Amato, G., Norell, M., DeSalle, R., Hayashi, C., 2003. Combined support for wholesale taxic atavism in gavialine crocodylians. Syst. Biol. 52, 403-422.

Gavryushkina, A., Welch, D., Stadler, T., Drummond, A.J., 2014. Bayesian inference of sampled ancestor trees for epidemiology and fossil calibration. PLoS Comput. Biol. 10, e1003919.

Gingerich, P.D. 1993. Oligocene age of the Gebel Qatrani Formation, Fayum, Egypt. J. Hum. Evol. 24, 207–218.

Goloboff, P.A., Catalano, S.A., 2016. TNT version 1.5, including a full implementation of phylogenetic morphometrics. Cladistics 32, 221-238.

Goloboff, P.A., Farris, J.S., Nixon, K.C., 2008. TNT, a free program for phylogenetic analysis. Cladistics 24, 774-786.

Goloboff, P.A., Pol, D., 2005. Parsimony and Bayesian phylogenetics. In: Albert, V.A. (Ed.), Parsimony, Phylogeny, and Genomics. Oxford University Press, New York, pp. 148–159.

Goloboff, P.A., Galvis, A.T., Arias, J.S., 2018a. Parsimony and model-based phylogenetic methods for morphological data: comments on O'Reilly et al. Palaeontology 61, 625-630.

Goloboff, P.A., Torres, A., Arias, J.S., 2018b. Weighted parsimony outperforms other methods of phylogenetic inference under models appropriate for morphology. Cladistics 34, 407-437.

Goloboff, P.A., Pittman, M., Pol, D., Xu, X., 2019. Morphological data sets fit a common mechanism much more poorly than DNA sequences and call into question the Mkv model. Syst. Biol. 68, 494-504.

Gradstein, F.M., Ogg, J.G., Schmitz, M.D., Ogg, G.M., 2012. The Geologic Time Scale 2012. Elsevier, Amsterdam.

Guillerme, T., Cooper, N., 2016. Effects of missing data on topological inference using a Total

Evidence approach. Mol. Phylogenet. Evol. 94, 146-158.

Gunnell, G.F., 2010. Chiroptera. In: Werdelin, L., Sanders, W.J. (Eds.), Cenozoic Mammals of Africa. University of California Press, Berkeley, pp. 587–603.

Gunnell, G.F., Gingerich, P.D., Holroyd, P.A. 2010. Ptolemaiida. In: Werdelin, L., Sanders, W.J. (Eds.), Cenozoic Mammals of Africa. University of California Press, Berkeley, pp. 83–87.

Gunnell, G.F., Boyer, D.M., Friscia, A.R., Heritage, S., Manthi, F.K., Miller, E.R., Sallam, H.M., Simmons, N.B., Stevens, N.J., Seiffert, E.R., 2018. Fossil lemurs from Egypt and Kenya suggest an African origin for Madagascar's aye-aye. Nat. Commun. 9, 3193.

Halenar, L.B., Cooke, S.B., Rosenberger, A.L., Rímoli, R., 2017. New cranium of the endemic Caribbean platyrrhine, *Antillothrix bernensis*, from La Altagracia Province, Dominican Republic. J. Hum. Evol. 106, 133–153.

Harrison, L.B., Larsson, H.C.E., 2015. Among-character rate variation distributions in phylogenetic analysis of discrete morphological characters. Syst. Biol. 64, 307–324.

Hasegawa, M., Kishino, H., Yano, T.-a., 1985. Dating of the human-ape splitting by a molecular clock of mitochondrial DNA. J. Mol. Evol. 22, 160-174.

Heath, T.A., Huelsenbeck, J.P., 2014. The fossilized birth–death process for coherent calibration of divergence-time estimates. Proc. Natl. Acad. Sci. USA 111, E2957–E2966.

Heritage, S., Seiffert, E.R., 2022. Total evidence time-scaled phylogenetic and biogeographic models for the evolution of sea cows (Sirenia, Afrotheria). PeerJ 10, e13886.

Hermsen, E.J., Hendricks, J.R., 2008. W(h)ither fossils? Studying morphological character evolution in the age of molecular sequences. Ann. Missouri Bot. Gard. 95, 72–100.

Hershkovitz, P., 1974. A new genus of late Oligocene monkey (Cebidae, Platyrrhini) with notes on postorbital closure and platyrrhine evolution. Folia Primatol. 21, 1–35.

Hillis, D.M., Bull, J.J., 1993. An empirical-test of bootstrapping as a method for assessing confidence in phylogenetic analysis. Syst. Biol. 42, 182-192.

Holder, M., Lewis, P.O., 2003. Phylogeny estimation: Traditional and Bayesian approaches. Nat. Rev. Genet. 4, 275-284.

Huelsenbeck, J.P., Ronquist, F., 2001. MRBAYES: Bayesian inference of phylogenetic trees. Bioinformatics 17, 754–755.

Huelsenbeck, J.P., Alfaro, M.E., Suchard, M.A., 2011. Biologically inspired phylogenetic models strongly outperform the no common mechanism model. Syst. Biol. 60, 225-232.

IUCN/SSC Primate Specialist Group - Taxonomy [WWW Document], n.d. http://www.primate-sg.org/taxonomy/ (accessed 4.11.22).

Jaeger, J.-J., Chavasseau, O., Lazzari, V., Naing Soe, A., Sein, C., Le Maître, A., Shwe, H., Chaimanee, Y., 2019. New Eocene primate from Myanmar shares dental characters with African Eocene crown anthropoids. Nat. Commun. 10, 3531.

Jansa, S.A., Barker, F.K., Voss, R.S., 2014. The early diversification history of didelphid marsupials: a window into South America's "Splendid Isolation." Evolution 68, 684–695.

Kay, R.F., 1990. The phyletic relationships of extant and fossil Pitheciinae (Platyrrhini, Anthropoidea). In: Fleagle, J.G., Rosenberger, A.L. (Eds.), The Platyrrhine Fossil Record. Academic Press, London. pp. 175–208.

Kay, R.F., 2010. A new primate from the early Miocene of Gran Barranca, Chubut Province, Argentina: Paleoecological implications. In: Madden, R.H., Carlini, A.A., Vucetich, M.G., Kay, R.F. (Eds.), The Paleontology of Gran Barranca: Evolution and Environmental Change through the Middle Cenozoic of Patagonia. Cambridge University Press, Cambridge. pp. 220–239.

Kay, R.F., 2015. Biogeography in deep time - What do phylogenetics, geology, and paleoclimate tell us about early platyrrhine evolution? Mol. Phylogen. Evol. 82, 358–374.

Kay, R.F., Madden, R.H., 1997. Mammals and rainfall: Paleoecology of the middle Miocene at La Venta (Colombia, South America). J. Hum. Evol. 32, 161–199.

Kay, R.F., Perry, J.M.G., 2019. New primates from the Río Santa Cruz and Río Bote (Early-Mid Miocene), Santa Cruz Province, Argentina. Publ. Electron. Aso. Paleontol. Argent. 19, 230-238.

Kay, R.F., Johnson, D., Meldrum, D.J., 1998a. A new pitheciin primate from the middle Miocene of Argentina. Am. J. Primatol. 45, 317–336.

Kay, R.F., Macfadden, B.J., Madden, R.H., Sandeman, H., Anaya, F., 1998b. Revised age of the Salla beds, Bolivia, and its bearing on the age of the Deseadan South American Land Mammal "Age." J. Vertebr. Paleontol. 18, 189–199.

Kay R.F., Madden R.H., Vucetich M.G., Carlini A.A., Mazzoni M.M., Re G.H., Heizler M., Sandeman H. 1999. Revised geochronology of the Casamayoran South American Land Mammal Age: climatic and biotic implications. Proc. Natl. Acad. Sci. USA 96, 13235-13240.

Kay, R.F., Fleagle, J.G., Mitchell, T.R.T., Colbert, M., Bown, T., Powers, D.W., 2008. The anatomy of *Dolichocebus gaimanensis*, a stem platyrrhine monkey from Argentina. J. Hum. Evol. 54, 323–382.

Kay, R.F., Perry, J.M.G., Malinzak, M.D., Allen, K.L., Kirk, E.C., Plavcan, J.M., Fleagle, J.G., 2012. The paleobiology of Santacrucian primates. In: Vizcaíno, S.F., Kay, R.F., Bargo, M.S. (Eds.), Early Miocene Paleobiology in Patagonia: High-Latitude Paleocommunities of the Santa Cruz Formation. Cambridge University Press, Cambridge, pp. 306–330.

Kay, R.F., Jeffrey Meldrum, D., Takai, M., 2013. Pitheciidae and other platyrrhine seed predators. In: Veiga, L.M., Barnett, A.A., Ferrari, S.F., Norconk, M.A. (Eds.), Evolutionary Biology and Conservation of Titis, Sakis and Uacaris. Cambridge University Press, Cambridge, pp. 3–12.

Kay, R.F., Gonzales, L.A., Salenbien, W., Martinez, J.-N., Cooke, S.B., Valdivia, L.A., Rigsby, C., Baker, P.A., 2019. *Parvimico materdei* gen. et sp. nov.: A new platyrrhine from the Early Miocene of the Amazon Basin, Peru. J. Hum. Evol. 134, 102628.

Kimura, M., 1980. A simple method for estimating evolutionary rates of base substitutions through comparative studies of nucleotide sequences. J. Mol. Evol. 16, 111-120.

King, B., 2019. Which morphological characters are influential in a Bayesian phylogenetic analysis? Examples from the earliest osteichthyans. Biol. Lett. 15, 20190288.

King, B., 2021. Bayesian tip-dated phylogenetics in paleontology: Topological effects and stratigraphic fit. Syst. Biol. 70, 283–294.

King, B., Beck, R.M.D., 2020. Tip dating supports novel resolutions of controversial relationships among early mammals. Proc. R. Soc. B Biol. Sci. 287, 20200943.

King, B., Qiao, T., Lee, M.S.Y., Zhu, M., Long, J.A., 2017. Bayesian morphological clock methods resurrect placoderm monophyly and reveal rapid early evolution in jawed vertebrates. Syst. Biol. 66, 499–516.

Kittel, R.N., Austin, A.D., Klopfstein, S., 2016. Molecular and morphological phylogenetics of chelonine parasitoid wasps (Hymenoptera: Braconidae), with a critical assessment of divergence time estimations. Mol. Phylogenet. Evol. 101, 224-241.

Klopfstein, S., Ryer, R., Coiro, M., Spasojevic, T., 2019. Mismatch of the morphology model is mostly unproblematic in total-evidence dating: Insights from an extensive simulation study.

bioRxiv preprint, 679084.

Kumar, S., Stecher, G., Li, M., Knyaz, C., Tamura, K., 2018. MEGA X: Molecular evolutionary genetics analysis across computing platforms. Mol. Biol. Evol. 35, 1547-1549.

Lanfear, R., Frandsen, P.B., Wright, A.M., Senfeld, T., Calcott, B., 2017. PartitionFinder 2: New methods for selecting partitioned models of evolution for molecular and morphological phylogenetic analyses. Mol. Biol. Evol. 34, 772–773.

Lawrence, B.N., Bennett, V.L., Churchill, J., Juckes, M., Kershaw, P., Pascoe, S., Pepler, S., Pritchard, M., Stephens, A., 2013. Storing and manipulating environmental big data with JASMIN. In: Proceedings of the 2013 IEEE International Conference on Big Data, Silicon Valley, CA, USA, pp. 68–75.

Lee, M.S.Y., 2020. Clock models for evolution of discrete phenotypic characters. In: Ho, S.Y.W. (Ed.), The Molecular Evolutionary Clock: Theory and Practice. Springer International Publishing, Cham, pp. 101–113.

Lee, M.S., Camens, A.B., 2009. Strong morphological support for the molecular evolutionary tree of placental mammals. J. Evol. Biol. 22, 2243-2257.

Lee, M.S., Worthy, T.H., 2012. Likelihood reinstates *Archaeopteryx* as a primitive bird. Biol. Lett. 8, 299-303.

Lee, M.S., Palci, A., 2015. Morphological phylogenetics in the genomic age. Curr. Biol. 25, R922-929.

Lee, M.S.Y., Yates, A.M., 2018. Tip-dating and homoplasy: Reconciling the shallow molecular divergences of modern gharials with their long fossil record. Proc. R. Soc. B Biol. Sci. 285, 20181071.

Lewis, P.O., 2001. A likelihood approach to estimating phylogeny from discrete morphological

character data. Syst. Biol. 50, 913–925.

López, M., García, M., Bucher, J., Funes, D.S., D'Elia, L., Bilmes, A., Naipauer, M., Sato, A.M., Valencia, V.A., Franzese, J.R., 2019. Structural evolution of The Collón Cura basin: Tectonic implications for the north Patagonian Broken Foreland. J. S. Am. Earth Sci. 93, 424–438.

Loss-Oliveira, L., Aguiar, B.O., Schrago, C.G., 2012. Testing synchrony in historical biogeography: The case of New World primates and Hystricognathi rodents. Evol. Bioinform. 8, 127–137.

Luo, A., Duchêne, D.A., Zhang, C., Zhu, C.-D., Ho, S.Y.W., 2019. A simulation-based evaluation of tip-dating under the fossilized birth–death process. Syst. Biol. 69, 325–344.

MacFadden, B.J., Bloch, J.I., Evans, H., Foster, D.A., Morgan, G.S., Rincon, A., Wood, A.R., 2014. Temporal calibration and biochronology of the Centenario Fauna, Early Miocene of Panama. J. Geol. 122, 113–135.

Madden, R.H., Guerrero, J., Kay, R.F., Flynn, J.J., Swisher, C.C., III, Walton, A.H., 1997. The Laventan Stage and Age. In: Kay, R.F., Madden, R.H., Cifelli, R.L., Flynn, J.J. (Eds.), Vertebrate Paleontology in the Neotropics: The Miocene Fauna of La Venta, Colombia. Smithsonian Institute Press, Washington, pp. 499–519.

MacPhee, R.D.E., Iturralde-Vinent, M.A., Gaffney, E.S., 2003. Domo de Zaza, an early Miocene vertebrate locality in south-central Cuba, with notes on the tectonic evolution of Puerto Rico and the Mona Passage. Am. Mus. Novit. 3394, 1-42.

Mammal Diversity Database, 2022. Mammal Diversity Database (Version 1.9). https://www.mammaldiversity.org/ (accessed 6.17.22).

Manos, P.S., Soltis, P.S., Soltis, D.E., Manchester, S.R., Oh, S.-H., Bell, C.D., Dilcher, D.L.,

Stone, D.E., Renner, S., 2007. Phylogeny of extant and fossil Juglandaceae inferred from the integration of molecular and morphological data sets. Syst. Biol. 56, 412-430.

Marivaux, L., Adnet, S., Altamirano-Sierra, A.J., Boivin, M., Pujos, F., Ramdarshan, A., Salas-Gismondi, R., Tejada-Lara, J.V., Antoine, P.-O., 2016a. Neotropics provide insights into the emergence of New World monkeys: New dental evidence from the late Oligocene of Peruvian Amazonia. J. Hum. Evol. 97, 159–175.

Marivaux, L., Adnet, S., Altamirano-Sierra, A.J., Pujos, F., Ramdarshan, A., Salas-Gismondi, R., Tejada-Lara, J.V., Antoine, P.-O., 2016b. Dental remains of cebid platyrrhines from the earliest late Miocene of Western Amazonia, Peru: Macroevolutionary implications on the extant capuchin and marmoset lineages. Am. J. Phys. Anthropol. 161, 478–493.

Marivaux, L., Aguirre-Diaz, W., Benites-Palomino, A., Billet, G., Boivin, M., Pujos, F., Salas-Gismondi, R., Tejada-Lara, J.V., Varas-Malca, R.M., Antoine, P.-O., 2020a. New record of *Neosaimiri* (Cebidae, Platyrrhini) from the late Middle Miocene of Peruvian Amazonia. J. Hum. Evol. 146, 102835.

Marivaux, L., Vélez-Juarbe, J., Merzeraud, G., Pujos, F., Viñola López, L.W., Boivin, M., Santos-Mercado, H., Cruz, E.J., Grajales, A., Padilla, J., Vélez-Rosado, K.I., Philippon, M., Léticée, J.-L., Münch, P., Antoine, P.-O., 2020b. Early Oligocene chinchilloid caviomorphs from Puerto Rico and the initial rodent colonization of the West Indies. Proc. R. Soc. B Biol. Sci. 287, 20192806.

Marshall, L.G., Pascual, R., Curtis, G.H., Drake, R.E., 1977. South American geochronology: Radiometric time scale for middle to late Tertiary mammal-bearing horizons in Patagonia. Science 195, 1325–1328.

Mather, E.K., Lee, M.S.Y., Camens, A.B., Worthy, T.H., 2021. An exceptional partial skeleton

of a new basal raptor (Aves: Accipitridae) from the late Oligocene Namba formation, South Australia. Hist. Biol. 34, 1175-1207.

Mazzoni MM, Benvenuto A. 1990. Radiometric ages of tertiary ignimbrites and the Collon Cura Formation, northwestern Patagonia. In: 9º Congreso Geológico Argentino, Actas, 2, 87–90.

Meredith, R.W., Janečka, J.E., Gatesy, J., Ryder, O.A., Fisher, C.A., Teeling, E.C., Goodbla, A., Eizirik, E., Simão, T.L.L., Stadler, T., Rabosky, D.L., Honeycutt, R.L., Flynn, J.J., Ingram, C.M., Steiner, C., Williams, T.L., Robinson, T.J., Burk-Herrick, A., Westerman, M., Ayoub, N.A., Springer, M.S., Murphy, W.J., 2011. Impacts of the Cretaceous Terrestrial Revolution and KPg extinction on mammal diversification. Science 334, 521–524.

Miller, K.G., Browning, J.V., Aubry, M.-P., Wade, B.S., Katz, M.E., Kulpecz, A.A., Wright, J.D., 2008. Eocene–Oligocene global climate and sea-level changes: St. Stephens Quarry, Alabama. Geol. Soc. Am. Bull. 120, 34–53.

Mitchell, K.J., Pratt, R.C., Watson, L.N., Gibb, G.C., Llamas, B., Kasper, M., Edson, J., Hopwood, B., Male, D., Armstrong, K.N., Meyer, M., Hofreiter, M., Austin, J., Donnellan, S.C., Lee, M.S.Y., Phillips, M.J., Cooper, A., 2014. Molecular phylogeny, biogeography, and habitat preference evolution of marsupials. Mol. Biol. Evol. 31, 2322–2330.

Mongiardino Koch, N., Garwood, R.J., Parry, L.A., 2021. Fossils improve phylogenetic analyses of morphological characters. Proc. R. Soc. B Biol. Sci. 288, 20210044.

Montes, C., Silva, C.A., Bayona, G.A., Villamil, R., Stiles, E., Rodriguez-Corcho, A.F., Beltran-Triviño, A., Lamus, F., Muñoz-Granados, M.D., Pérez-Angel, L.C., Hoyos, N., Gomez, S., Galeano, J.J., Romero, E., Baquero, M., Cardenas-Rozo, A.L., von Quadt, A., 2021. A middle to late Miocene trans-Andean portal: Geologic record in the Tatacoa Desert. Front. Earth Sci. 8, 643.

Morse, P.E., Chester, S.G.B., Boyer, D.M., Smith, T., Smith, R., Gigase, P., Bloch, J.I., 2019. New fossils, systematics, and biogeography of the oldest known crown primate Teilhardina from the earliest Eocene of Asia, Europe, and North America. J. Hum. Evol. 128, 103-131.

Neumann, J.S., Desalle, R., Narechania, A., Schierwater, B., Tessler, M., 2021. Morphological characters can strongly influence early animal relationships inferred from phylogenomic data sets. Syst. Biol. 70, 360-375.

Ni, X., Flynn, J.J., Wyss, A.R., Zhang, C., 2019. Cranial endocast of a stem platyrrhine primate and ancestral brain conditions in anthropoids. Sci. Adv. 5, eaav7913.

Nivière, B., Huyghe, D., Bonnel, C., Lacan, P., 2019. Neogene sedimentation and tectonics in the Collón Curá basin (Patagonian Andes of Argentina). J. S. Am. Earth Sci. 96, 102244.

Novo, N.M., Tejedor, M.F., Pérez, M.E., Krause, J.M., 2017. New primate locality from the early Miocene of Patagonia, Argentina. Am. J. Phys. Anthropol. 164, 861-867.

Novo, N.M., Tejedor, M.F., González-Ruiz, L.R., Fleagle, J.G., Brandoni, D., Krause, M., 2021. Primate diversity in the early Miocene Pinturas Formation, southern Patagonia, Argentina. An. Acad. Bras. Cienc. 93, e20201218.

O'Reilly, J.E., Donoghue, P.C.J., 2016. Tips and nodes are complementary not competing approaches to the calibration of molecular clocks. Biol. Lett. 12, 20150975.

O'Reilly, J.E., Donoghue, P.C.J., 2018. The efficacy of consensus tree methods for summarizing phylogenetic relationships from a posterior sample of trees estimated from morphological data. Syst. Biol. 67, 354–362.

O'Reilly, J.E., Donoghue, P.C.J., 2019. The effect of fossil sampling on the estimation of divergence times with the fossilized birth–death process. Syst. Biol. 69, 124–138.

O'Reilly, J.E., Dos Reis, M., Donoghue, P.C.J., 2015. Dating tips for divergence-time

estimation. Trends Genet. 31, 637–650.

O'Reilly, J.E., Puttick, M.N., Parry, L., Tanner, A.R., Tarver, J.E., Fleming, J., Pisani, D., Donoghue, P.C.J., 2016. Bayesian methods outperform parsimony but at the expense of precision in the estimation of phylogeny from discrete morphological data. Biol. Lett. 12, 20160081.

O'Reilly, J.E., Puttick, M.N., Pisani, D., Donoghue, P.C.J., 2018a. Probabilistic methods surpass parsimony when assessing clade support in phylogenetic analyses of discrete morphological data. Palaeontology 61, 105-118.

O'Reilly, J.E., Puttick, M.N., Pisani, D., Donoghue, P.C.J., Smith, A., 2018b. Empirical realism of simulated data is more important than the model used to generate it: A reply to Goloboff et al. Palaeontology 61, 631-635.

Paradis, E., Schliep, K., 2019. ape 5.0: An environment for modern phylogenetics and evolutionary analyses in R. Bioinformatics 35, 526–528.

Parins-Fukuchi, C., Brown, J.W., 2017. What drives results in Bayesian morphological clock analyses? bioRxiv preprint, 219048.

Perelman, P., Johnson, W.E., Roos, C., Seuánez, H.N., Horvath, J.E., Moreira, M.A.M., Kessing, B., Pontius, J., Roelke, M., Rumpler, Y., Schneider, M.P.C., Silva, A., O'Brien, S.J., Pecon-Slattery, J., 2011. A molecular phylogeny of living primates. PLoS Genet. 7, e1001342.

Perkins, M.E., Fleagle, J.G., Heizler, M.T., Nash, B., Bown, T.M., Tauber, A.A., Dozo, M.T., 2012. Tephrochronology of the Miocene Santa Cruz and Pinturas Formations, Argentina. In: Vizcaíno, S.F., Kay, R.F., Bargo, M.S. (Eds.), Early Miocene Paleobiology in Patagonia: High-Latitude Paleocommunities of the Santa Cruz Formation. Cambridge University Press, Cambridge, pp. 23–40.

Poux, C., Chevret, P., Huchon, D., de Jong, W.W., Douzery, E.J.P., 2006. Arrival and diversification of caviomorph rodents and platyrrhine primates in South America. Syst. Biol. 55, 228–244.

Prevosti, F.J., Forasiepi, A.M., 2018. Evolution of South American Mammalian Predators During the Cenozoic: Paleobiogeographic and Paleoenvironmental Contingencies. Springer, Cham.

Prevosti, F.J., Romano, C.O., Forasiepi, A.M., Hemming, S., Bonini, R., Candela, A.M., Cerdeño, E., Madozzo Jaén, M.C., Ortiz, P.E., Pujos, F., Rasia, L., Schmidt, G.I., Taglioretti, M., MacPhee, R.D.E., Pardiñas, U.F.J., 2021. New radiometric 40Ar–39Ar dates and faunistic analyses refine evolutionary dynamics of Neogene vertebrate assemblages in southern South America. Sci. Rep. 11, 9830.

Pugh, K.D., 2022. Phylogenetic analysis of Middle-Late Miocene apes. J. Hum. Evol. 165, 103140.

Püschel, H.P., O'Reilly, J.E., Pisani, D., Donoghue, P.C.J., 2020. The impact of fossil stratigraphic ranges on tip- calibration, and the accuracy and precision of divergence time estimates. Palaeontology 63, 67–83.

Puttick, M.N., Thomas, G.H., Benton, M.J., 2016. Dating Placentalia: Morphological clocks fail to close the molecular fossil gap. Evolution 70, 873–886.

Puttick, M.N., O'Reilly, J.E., Pisani, D., Donoghue, P.C.J., Rahman, I., 2019. Probabilistic methods outperform parsimony in the phylogenetic analysis of data simulated without a probabilistic model. Palaeontology 62, 1-17.

Pyron, R.A., 2011. Divergence time estimation using fossils as terminal taxa and the origins of Lissamphibia. Syst. Biol. 60, 466–481.

Raffi, I., Wade, B.S., Pälike, H., Beu, A.G., Cooper, R., Crundwell, M.P., Krijgsman, W., Moore, T., Raine, I., Sardella, R., Vernyhorova, Y.V., 2020. The Neogene period. In: Gradstein, F.M., Ogg, J.G., Schmitz, M.D., Ogg, G.M. (Eds.), Geologic Time Scale 2020. Elsevier, Amsterdam, pp. 1141–1215.

Rambaut, A., Drummond, A.J., Xie, D., Baele, G., Suchard, M.A., 2018. Posterior summarization in Bayesian phylogenetics using Tracer 1.7. Syst. Biol. 67, 901–904.

Ré, G.H., Geuna, S.E., Vilas, J.F., Madden, R.H., Carlini, A.A., Vucetich, M.G., Kay, R.F., 2010. Paleomagnetism and magnetostratigraphy of Sarmiento Formation (Eocene-Miocene) at Gran Barranca, Chubut, Argentina. In: Madden, R.H., Carlini, A.A., Vucetich, M.G., Kay, R.F. (Eds.), The Paleontology of Gran Barranca: Evolution and Environmental Change through the Middle Cenozoic of Patagonia. Cambridge University Press, Cambridge, pp. 32–58.

Rímoli, R., 1977. Una nueva especie de monos (Cebidae: Saimirinae: Saimiri) de la Hispaniola. Cuadernos del Centro Dominicano de investigaciones antropológicas (CENDIA). Universidad Autónoma de Santa Domingo 242, 1–14.

Rivero, M., Arredondo, O., 1991. Paralouatta varonai, a new Quaternary platyrrhine from Cuba. J. Hum. Evol. 21, 1–11.

Ronquist, F., Klopfstein, S., Vilhelmsen, L., Schulmeister, S., Murray, D.L., Rasnitsyn, A.P., 2012a. A total-evidence approach to dating with fossils, applied to the early radiation of the Hymenoptera. Syst. Biol. 61, 973–999.

Ronquist, F., Teslenko, M., van der Mark, P., Ayres, D.L., Darling, A., Höhna, S., Larget, B., Liu, L., Suchard, M.A., Huelsenbeck, J.P., 2012b. MrBayes 3.2: Efficient Bayesian phylogenetic inference and model choice across a large model space. Syst. Biol. 61, 539–

542.

Ronquist, F., Lartillot, N., Phillips, M.J., 2016. Closing the gap between rocks and clocks using total-evidence dating. Phil. Trans. R. Soc. B Biol. Sci. 371, 20150136.

Rosenberger, A.L., 2010. Platyrrhines, PAUP, parallelism, and the Long Lineage Hypothesis: A reply to Kay et al. (2008). J. Hum. Evol. 59, 218–222.

Rosenberger, A.L., 2011. Evolutionary morphology, platyrrhine evolution, and systematics. Anat. Rec. 294, 1955–1974.

Rosenberger, A.L., 2019. *Dolichocebus gaimanensis* is not a stem platyrrhine. Folia Primatol. 90, 494–506.

Rosenberger, A.L., 2020. New World Monkeys: The Evolutionary Odyssey. Princeton University Press, Princeton.

Rosenberger, A.L., Tejedor, M.F., 2013. The misbegotten: Long lineages, long branches and the interrelationships of *Aotus*, *Callicebus* and the saki-uacaris. In: Veiga, L.M., Barnett, A.A., Ferrari, S.F., Norconk, M.A. (Eds.), Evolutionary Biology and Conservation of Titis, Sakis and Uacaris. Cambridge University Press, Cambridge, pp. 13–22.

Rosenberger, A.L., Hartwig, W.C., Takai, M., Setoguchi, T., Shigehara, N., 1991. Dental variability in *Saimiri* and the taxonomic status of *Neosaimiri fieldsi*, an early squirrel monkey from La Venta, Colombia. Int. J. Primatol. 12, 291–301.

Rosenberger, A.L., Tejedor, M.F., Cooke, S.B., Pekar, S., 2009. Platyrrhine ecophylogenetics in space and time. In: Garber, P.A., Estrada, A., Bicca-Marques, J.C., Heymann, E.W., Strier, K.B. (Eds.), South American Primates: Comparative Perspectives in the Study of Behavior, Ecology, and Conservation. Springer New York, New York, NY, pp. 69–113.

Rosenberger, A.L., Cooke, S.B., Rímoli, R., Ni, X., Cardoso, L., 2011. First skull of *Antillothrix*

bernensis, an extinct relict monkey from the Dominican Republic. Proc. R. Soc. B Biol. Sci. 278, 67–74.

Rosenberger, A.L., Pickering, R., Green, H., Cooke, S.B., Tallman, M., Morrow, A., Rímoli, R., 2015. 1.32±0.11 Ma age for underwater remains constrain antiquity and longevity of the Dominican primate *Antillothrix bernensis*. J. Hum. Evol. 88, 85–96.

Rowe, D.L., Dunn, K.A., Adkins, R.M., Honeycutt, R.L., 2010. Molecular clocks keep dispersal hypotheses afloat: Evidence for trans-Atlantic rafting by rodents. J. Biogeogr. 37, 305–324.

Sallam, H.M., Seiffert, E.R., 2020. Revision of Oligocene "*Paraphiomys*" and an origin for crown Thryonomyoidea (Rodentia: Hystricognathi: Phiomorpha) near the Oligocene--Miocene boundary in Africa. Zool. J. Linn. Soc. 190, 352–371.

Sallam, H.M., Seiffert, E.R., Steiper, M.E., Simons, E.L., 2009. Fossil and molecular evidence constrain scenarios for the early evolutionary and biogeographic history of hystricognathous rodents. Proc. Natl. Acad. Sci. USA 106, 16722–16727.

Schneider, H., Sampaio, I., 2015. The systematics and evolution of New World primates—A review. Mol. Phylogen. Evol. 82, 348–357.

Schrago, C.G., Seuánez, H.N., 2019. Large ancestral effective population size explains the difficult phylogenetic placement of owl monkeys. Am. J. Primatol. 81, e22955.

Schrago, C.G., Mello, B., Soares, A.E.R., 2013. Combining fossil and molecular data to date the diversification of New World primates. J. Evol. Biol. 26, 2438–2446.

Seiffert, E.R., 2006. Revised age estimates for the later Paleogene mammal faunas of Egypt and Oman. Proc. Natl. Acad. Sci. USA 103, 5000–5005.

Seiffert, E.R., 2010. Chronology of Paleogene mammal localities. In: Werdelin, L., Sanders, W.J. (Eds.), Cenozoic Mammals of Africa. University of California Press, Berkeley, pp. 19–

26.

Seiffert, E.R., Simons, E.L., Fleagle, J.G., Godinot, M., 2010. Paleogene anthropoids. In: Werdelin, L., Sanders, W.J. (Eds.), Cenozoic Mammals of Africa. University of California Press, Berkeley, pp. 369–392.

Seiffert, E.R., Tejedor, M.F., Fleagle, J.G., Novo, N.M., Cornejo, F.M., Bond, M., de Vries, D., Campbell, K.E., Jr, 2020. A parapithecid stem anthropoid of African origin in the Paleogene of South America. Science 368, 194–197.

Silvestro, D., Tejedor, M.F., Serrano-Serrano, M.L., Loiseau, O., Rossier, V., Rolland, J., Zizka, A., Höhna, S., Antonelli, A., Salamin, N., 2019. Early arrival and climatically-linked geographic expansion of New World monkeys from tiny African ancestors. Syst. Biol. 68, 78–92.

Simmons, M.P., 2014. A confounding effect of missing data on character conflict in maximum likelihood and Bayesian MCMC phylogenetic analyses. Mol. Phylogenet. Evol. 80, 267–280.

Simões, T.R., Caldwell, M.W., Pierce, S.E., 2020. Sphenodontian phylogeny and the impact of model choice in Bayesian morphological clock estimates of divergence times and evolutionary rates. BMC Biol. 18, 191.

Smith, M.R., 2019. Bayesian and parsimony approaches reconstruct informative trees from simulated morphological datasets. Biol. Lett. 15, 20180632.

Smith, M.R., 2021. Using information theory to detect rogue taxa and improve consensus trees. Syst. Biol. 71, 1088-1094.

Smith, M.R., 2022. Rogue: Identify rogue taxa in sets of phylogenetic trees. Comprehensive R Archive Network (CRAN). https://CRAN.R-project.org/package=Rogue.

Speijer, R.P., Pälike, H., Hollis, C.J., Hooker, J.J., Ogg, J.G., 2020. The Paleogene Period. In: Gradstein, F.M., Ogg, J.G., Schmitz, M.D., Ogg, G.M. (Eds.), Geologic Time Scale 2020. Elsevier, Amsterdam, pp. 1087–1140.

Springer, M.S., Meredith, R.W., Gatesy, J., Emerling, C.A., Park, J., Rabosky, D.L., Stadler, T., Steiner, C., Ryder, O.A., Janečka, J.E., Fisher, C.A., Murphy, W.J., 2012. Macroevolutionary dynamics and historical biogeography of primate diversification inferred from a species supermatrix. PLoS One 7, e49521.

Stadler, T., 2010. Sampling-through-time in birth–death trees. J. Theor. Biol. 267, 396–404.

Stamatakis, A., 2014. RAxML version 8: A tool for phylogenetic analysis and post-analysis of large phylogenies. Bioinformatics 30, 1312–1313.

Steiner, C., Tilak, M.-K., Douzery, E.J.P., Catzeflis, F.M., 2005. New DNA data from a transthyretin nuclear intron suggest an Oligocene to Miocene diversification of living South America opossums (Marsupialia: Didelphidae). Mol. Phylogen. Evol. 35, 363–379.

Takai, M., 1994. New specimens of Neosaimiri fieldsi from La Venta, Colombia: A middle Miocene ancestor of the living squirrel monkeys. J. Hum. Evol. 27, 329–360.

Tejedor, M.F., Novo, N.M., 2016. Evolución y paleobiogeografía de los primates platirrinos. In: Agnolin, F.L., Lio, G.L., Brissón Egli, F., Chimento, N.R., Novas, F.E. (Eds.), Historia Evolutiva Y Paleobiogeográfica de Los Vertebrados de América Del Sur. Museo Argentino de Ciencias Naturales “Bernardino Rivadavia,” Buenos Aires, pp. 385–393.

Trayler, R.B., Schmitz, M.D., Cuitiño, J.I., Kohn, M.J., Bargo, M.S., Kay, R.F., Strömberg, C.A.E., Vizcaíno, S.F., 2020. An improved approach to age-modeling in deep time: Implications for the Santa Cruz Formation, Argentina. Geol. Soc. Am. Bull. 132, 233-244.

Turner, A.H., Pritchard, A.C., Matzke, N.J., 2017. Empirical and Bayesian approaches to fossil-

only divergence times: A study across three reptile clades. PLoS One 12, e0169885.

Upham, N.S., Patterson, B.D., 2012. Diversification and biogeography of the Neotropical caviomorph lineage Octodontoidea (Rodentia: Hystricognathi). Mol. Phylogen. Evol. 63, 417–429.

Upham, N.S., Patterson, B.D., 2015. Evolution of caviomorph rodents: A complete phylogeny and timetree for living genera. In: Vassallo, A.I., Antenucci, D. (Eds.), Biology of Caviomorph Rodents: Diversity and Evolution. SAREM Series A, Buenos Aires, pp. 63–120.

Van Couvering, J.A., Delson, E., 2020. African Land Mammal Ages. J. Vertebr. Paleontol. 40, e1803340.

Vanderpool, D., Minh, B.Q., Lanfear, R., Hughes, D., Murali, S., Harris, R.A., Raveendran, M., Muzny, D.M., Hibbins, M.S., Williamson, R.J., Gibbs, R.A., Worley, K.C., Rogers, J., Hahn, M.W., 2020. Primate phylogenomics uncovers multiple rapid radiations and ancient interspecific introgression. PLoS Biol. 18, e3000954.

Vilela, J.F., Alves de Oliveira, J., Russo, C.A. de M., 2015. The diversification of the genus *Monodelphis* and the chronology of Didelphidae (Didelphimorphia). Zool. J. Linn. Soc. 174, 414–427.

Villarroael A, C., Setoguchi, T., Brieva, J., Macia, C., 1996. Geology of the La Tatacoa “desert” (Huila, Colombia): Precisions on the stratigraphy of the Honda group, the evolution of the “Pata high” and the presence of the La Venta fauna. Memoirs of the Faculty of Science, Kyoto University. Ser. Geol. Mineral. 58, 41–66.

Voloch, C.M., Vilela, J.F., Loss-Oliveira, L., Schrago, C.G., 2013. Phylogeny and chronology of the major lineages of New World hystricognath rodents: Insights on the biogeography of the

Eocene/Oligocene arrival of mammals in South America. BMC Res. Notes 6, 160.

Wang, X., Lim, B.K., Ting, N., Hu, J., Liang, Y., Roos, C., Yu, L., 2019. Reconstructing the phylogeny of New World monkeys (Platyrrhini): Evidence from multiple non-coding loci. Curr. Zool. 65, 579–588.

Welker, F., Ramos-Madrigal, J., Kuhlwilm, M., Liao, W., Gutenbrunner, P., de Manuel, M., Samodova, D., Mackie, M., Allentoft, M.E., Bacon, A.-M., Collins, M.J., Cox, J., Lalueza-Fox, C., Olsen, J.V., Demeter, F., Wang, W., Marques-Bonet, T., Cappellini, E., 2019. Enamel proteome shows that *Gigantopithecus* was an early diverging pongine. Nature 576, 262–265.

Welker, F., Ramos-Madrigal, J., Gutenbrunner, P., Mackie, M., Tiwary, S., Rakownikow Jersie-Christensen, R., Chiva, C., Dickinson, M.R., Kuhlwilm, M., de Manuel, M., Gelabert, P., Martinón-Torres, M., Margvelashvili, A., Arsuaga, J.L., Carbonell, E., Marques-Bonet, T., Penkman, K., Sabidó, E., Cox, J., Olsen, J.V., Lordkipanidze, D., Racimo, F., Lalueza-Fox, C., Bermúdez de Castro, J.M., Willerslev, E., Cappellini, E., 2020. The dental proteome of *Homo antecessor*. Nature 580, 235–238.

Wiens, J.J., 2009. Paleontology, genomics, and combined-data phylogenetics: Can molecular data improve phylogeny estimation for fossil taxa? Syst. Biol. 58, 87-99.

Wiens, J.J., Moen, D.S., 2008. Missing data and the accuracy of Bayesian phylogenetics. J. Syst. Evol. 46, 307-314.

Wiens, J.J., Tiu, J., 2012. Highly incomplete taxa can rescue phylogenetic analyses from the negative impacts of limited taxon sampling. PLoS One 7, e42925.

Wisniewski, A.L., Lloyd, G.T., Slater, G.J., 2022. Extant species fail to estimate ancestral geographical ranges at older nodes in primate phylogeny. Proc. R. Soc. B Biol. Sci. 289,

20212535.

Woods, R., Turvey, S.T., Brace, S., MacPhee, R.D.E., Barnes, I., 2018. Ancient DNA of the extinct Jamaican monkey *Xenothrix* reveals extreme insular change within a morphologically conservative radiation. Proc. Natl. Acad. Sci. USA 115, 12769–12774.

Woods, R., Barnes, I., Brace, S., Turvey, S.T., 2021. Ancient DNA suggests single colonization and within-archipelago diversification of Caribbean caviomorph rodents. Mol. Biol. Evol. 38, 84–95.

Wright, A.M., Hillis, D.M., 2014. Bayesian analysis using a simple likelihood model outperforms parsimony for estimation of phylogeny from discrete morphological data. PLoS One 9, e109210.

Wyss, A.R., Norell, M.A., Flynn, J.J., Novacek, M.J., Charrier, R., Mckenna, M.C., Swisher, C.C., Frassinetti, D., Salinas, P., Jin, M., 1990. A new early Tertiary mammal fauna from central Chile: Implications for Andean stratigraphy and tectonics. J. Vertebr. Paleontol. 10, 518–522.

Wyss, A.R., Flynn, J.J., Norell, M.A., Swisher, C.C., Charrier, R., Novacek, M.J., McKenna, M.C., 1993. South America's earliest rodent and recognition of a new interval of mammalian evolution. Nature 365, 434–437.

Xu, X., Pol, D., 2013. *Archaeopteryx*, paravian phylogenetic analyses, and the use of probability-based methods for palaeontological datasets. J. Syst. Palaeontol. 12, 323-334.

Yang, Z., Rannala, B., 2012. Molecular phylogenetics: Principles and practice. Nat. Rev. Genet. 13, 303-314.

Zhang, C., Stadler, T., Klopfstein, S., Heath, T.A., Ronquist, F., 2016. Total-evidence dating under the fossilized birth-death process. Syst. Biol. 65, 228–249.

Figure legends

Figure 1. 50% majority rule consensus of post-burn-in trees that results from undated Bayesian analysis of the molecular sequence dataset (17 nuclear loci, 10.2 kb) using MrBayes v. 3.2.7a. Support values at nodes are Bayesian posterior probabilities.

Figure 2. Strict consensus of four most parsimonious trees (length = 1829 steps) from maximum parsimony analysis of the morphological dataset (418 characters) using TNT v. 1.5. Support values at nodes are bootstrap values (based on 2000 replicates); nodes without support values were constrained to be monophyletic a priori (see Methods for further details).

Figure 3. Results from undated Bayesian analysis of the morphological dataset (418 characters) using MrBayes v. 3.2.7a. A) 50% majority rule consensus of post-burn-in trees with all taxa included. B) 50% majority rule consensus of post-burn-in trees after a posteriori pruning of unstable taxa (indicated by * in A) identified by Rogue v. 2.1.0 (see Table 3). Support values at nodes are Bayesian posterior probabilities; nodes without support values were constrained to be monophyletic a priori (see Methods for further details).

Figure 4. Results from maximum parsimony analysis of the morphological dataset (418 characters) with the molecular scaffold of Kay et al. (2019) enforced as a backbone constraint, using TNT v. 1.5. A) Strict consensus of three most parsimonious trees (length = 1877 steps) with all taxa included. B) Strict consensus of three most parsimonious trees (length = 1877 steps) after a posteriori pruning of a single unstable taxon (*Cebupithecia*, indicated by * in A) identified by Rogue v. 2.1.0 (see Table 3). Support values at nodes are bootstrap values (based on 2000 replicates); nodes without support values were constrained to be monophyletic a priori (see Methods for further details).

Figure 5. Results from undated Bayesian analysis of the morphological dataset (418 characters) with the molecular scaffold of Kay et al. (2019) enforced as a backbone constraint, using MrBayes v. 3.2.7a. A) 50% majority rule consensus of post-burn-in trees with all taxa included. B) 50% majority rule consensus of post-burn-in trees after a posteriori pruning of unstable taxa (indicated by * in A) identified by Rogue v. 2.1.0 (see Table 3). Support values at nodes are Bayesian posterior probabilities; nodes without support values were constrained to be monophyletic a priori (see Methods for further details).

Figure 6. Results from undated Bayesian analysis of the total evidence dataset using MrBayes v. 3.2.7a. A) 50% majority rule consensus of post-burn-in trees including all taxa. B) 50% majority rule consensus of post-burn-in trees after a posteriori pruning of unstable taxa (indicated by * in A) identified by Rogue v. 2.1.0. Support values at nodes are Bayesian posterior probabilities; nodes without support values were constrained to be monophyletic a priori (see Methods for further details).

Figure 7. Results from tip-dating Bayesian analysis of the total evidence dataset using MrBayes v. 3.2.7a. A) 'Allcompat' majority rule consensus of post-burn-in trees including all taxa. B) 'Allocompat' majority rule consensus of post-burn-in trees after a posteriori pruning of unstable taxa (indicated by * in A) identified by Rogue v. 2.1.0. Support values at nodes are Bayesian posterior probabilities (BPPs); nodes without support values were constrained to be monophyletic a priori (see Methods for further details), or have BPP of <0.5. Branches represented by dotted lines lead to nodes with BPPs of <0.5, and so collapse in a 50% majority rule consensus. Divergence dates are median posterior estimates, and blue bars are 95% highest posterior density intervals. Eo. = Eocene, Ol. = Oligocene, P. = Pliocene, Pa. = Paleogene, Pl. = Pleistocene + Holocene, Q. = Quaternary.

Figure 1

Click here to access/download;Figure;Fig1_molec_tr_no_layers.tif

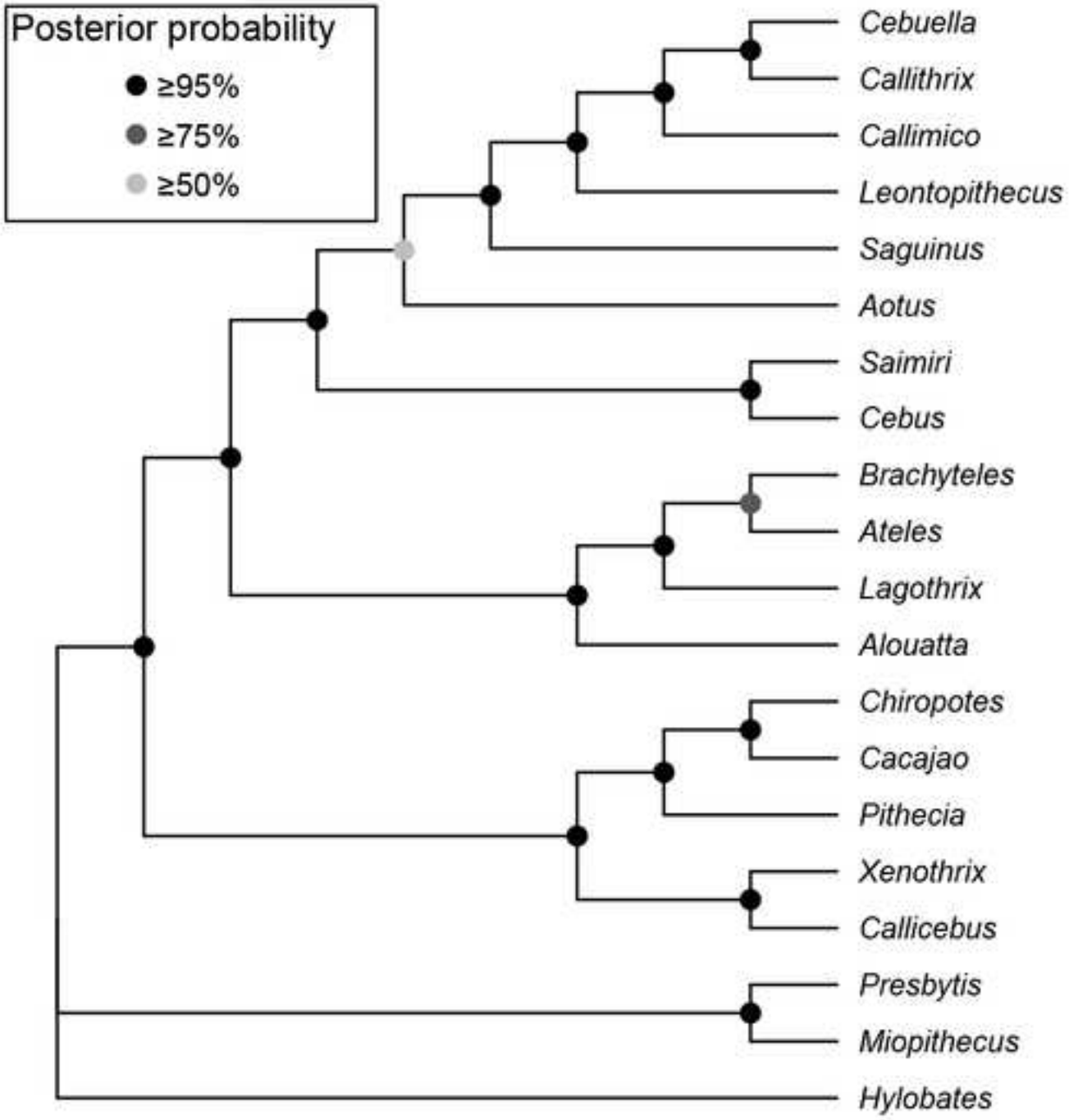

Figure 2

Click here to access/download;Figure;Fig2_Morph_strict_MP_tr_no_layers.tif

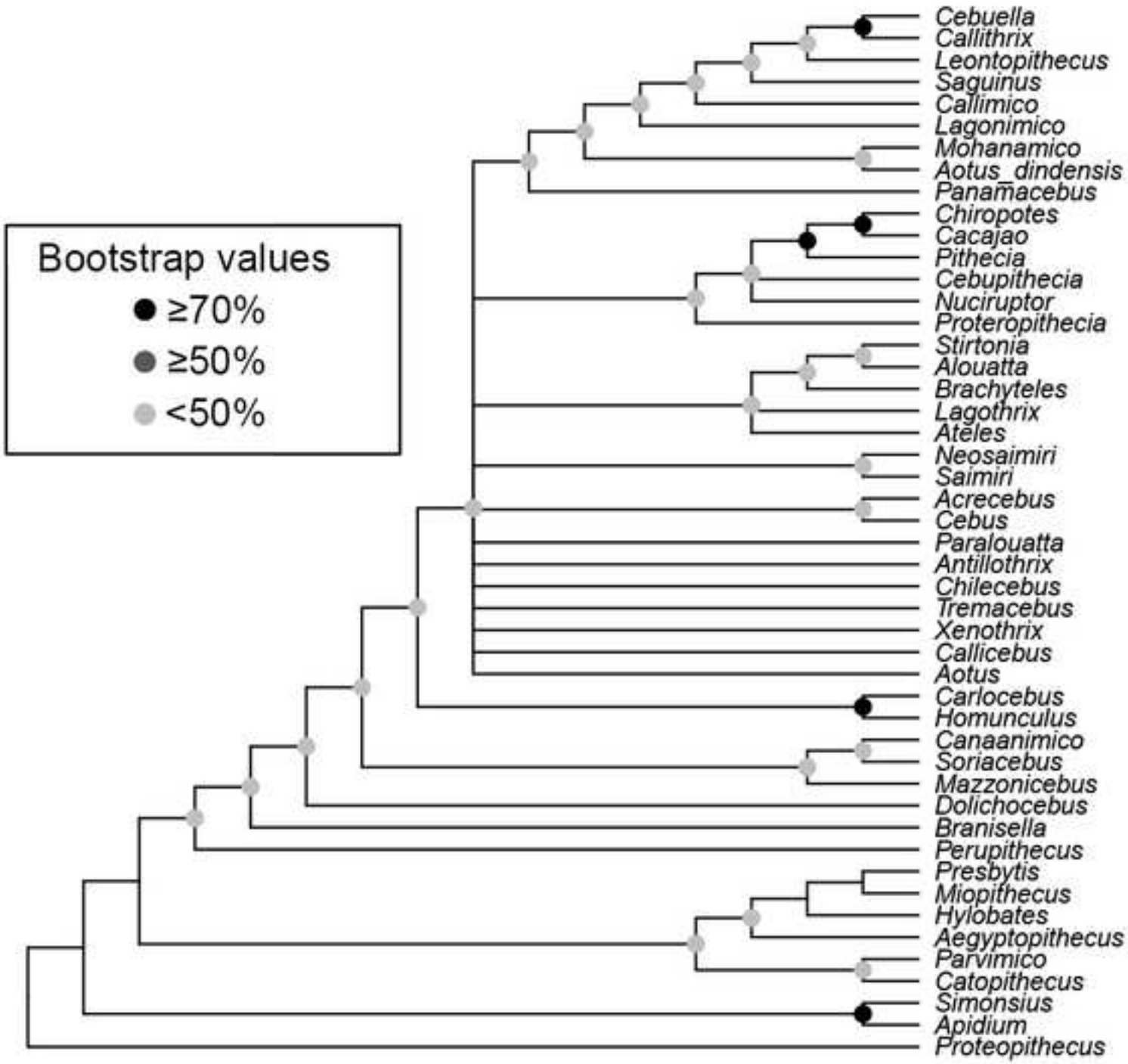

Figure 3

Click here to access/download;Figure;Fig3_morph_Bayes_tr_no_layers.tif

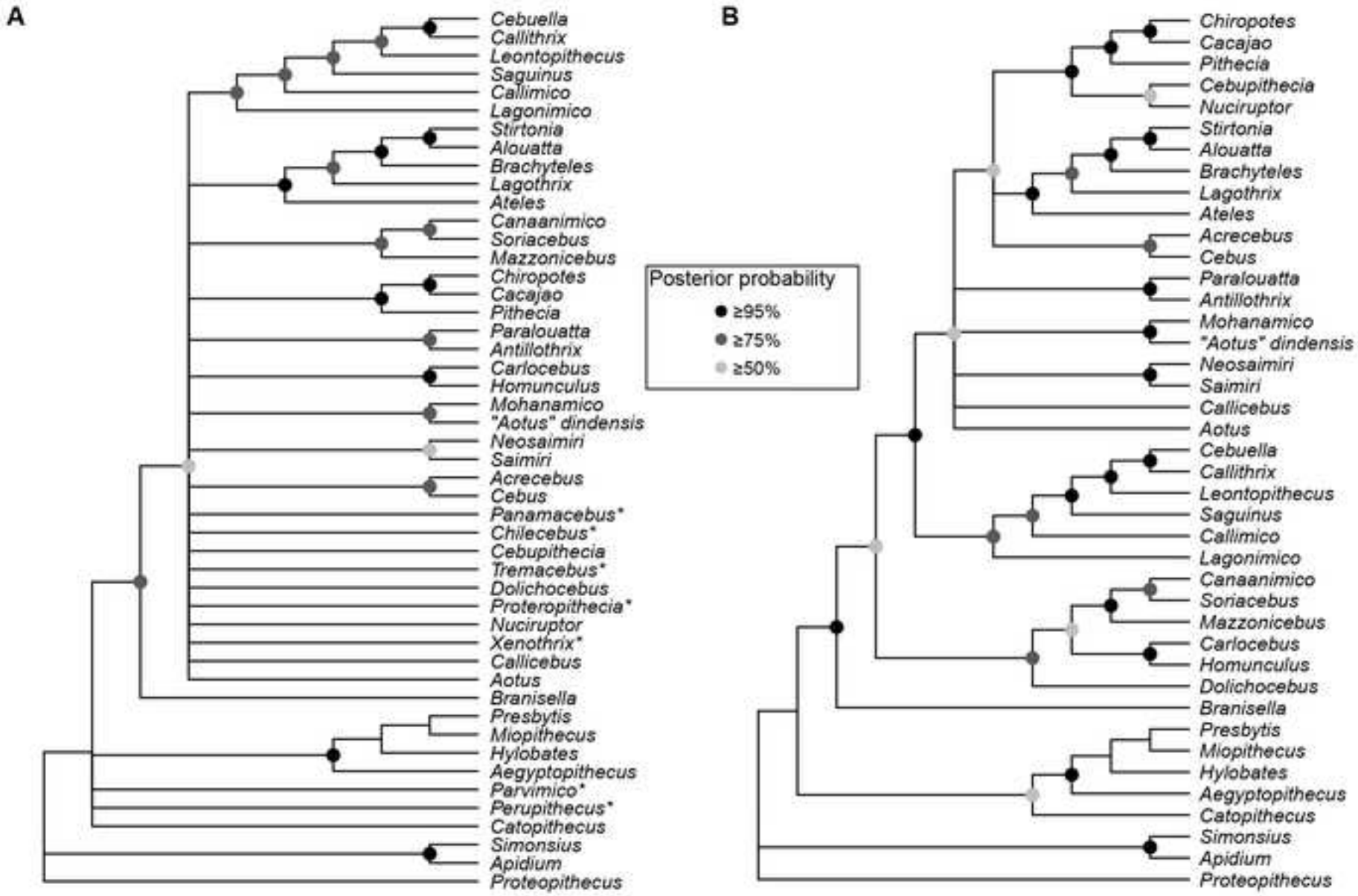

Figure 5

Click here to access/download;Figure;Fig5_morph_scaffold_Bayes_NEW_no_layers.tif

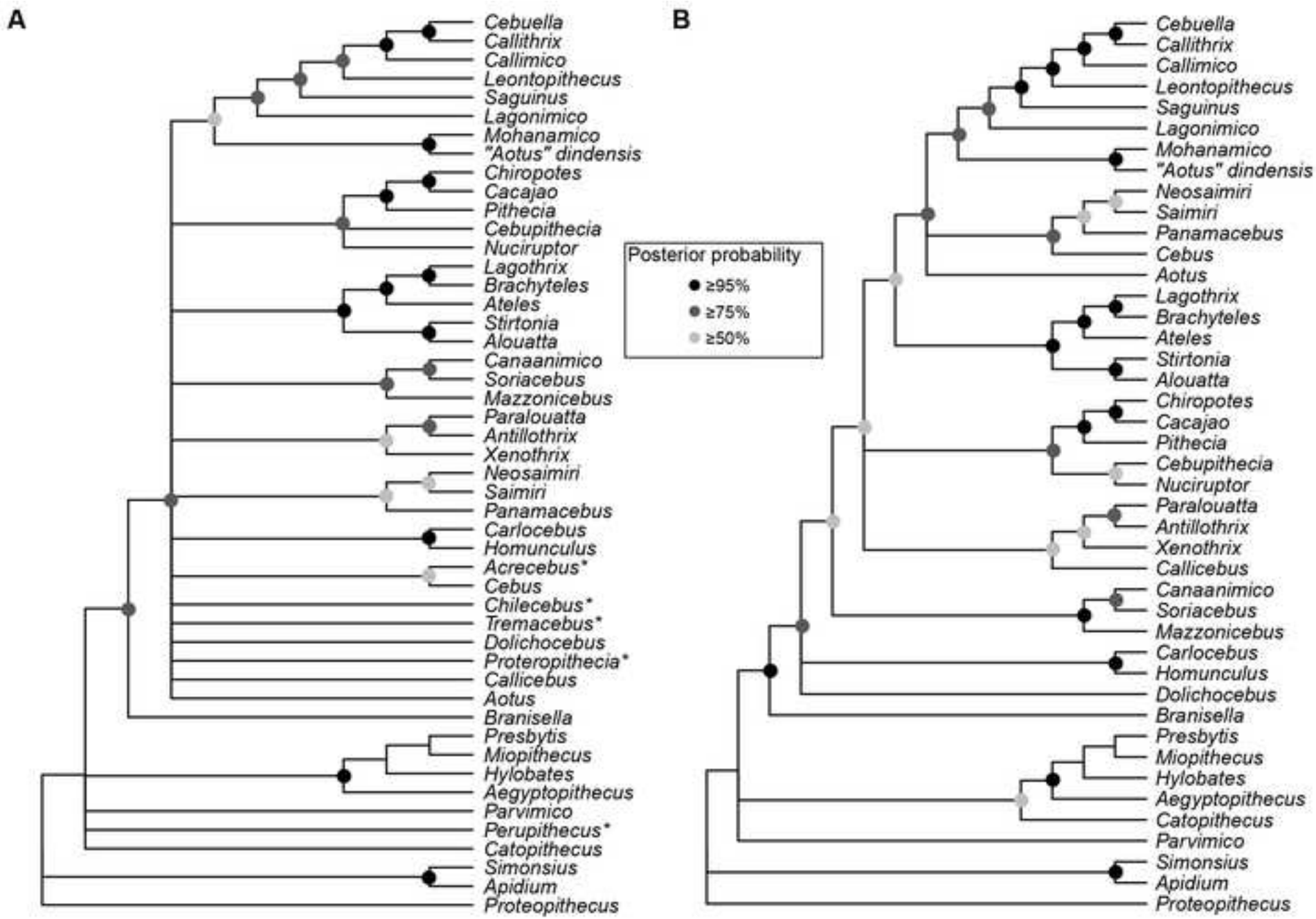

Figure 4

Click here to access/download;Figure;Fig4_morph_scaffold_MP_NEW_no_layers.tif

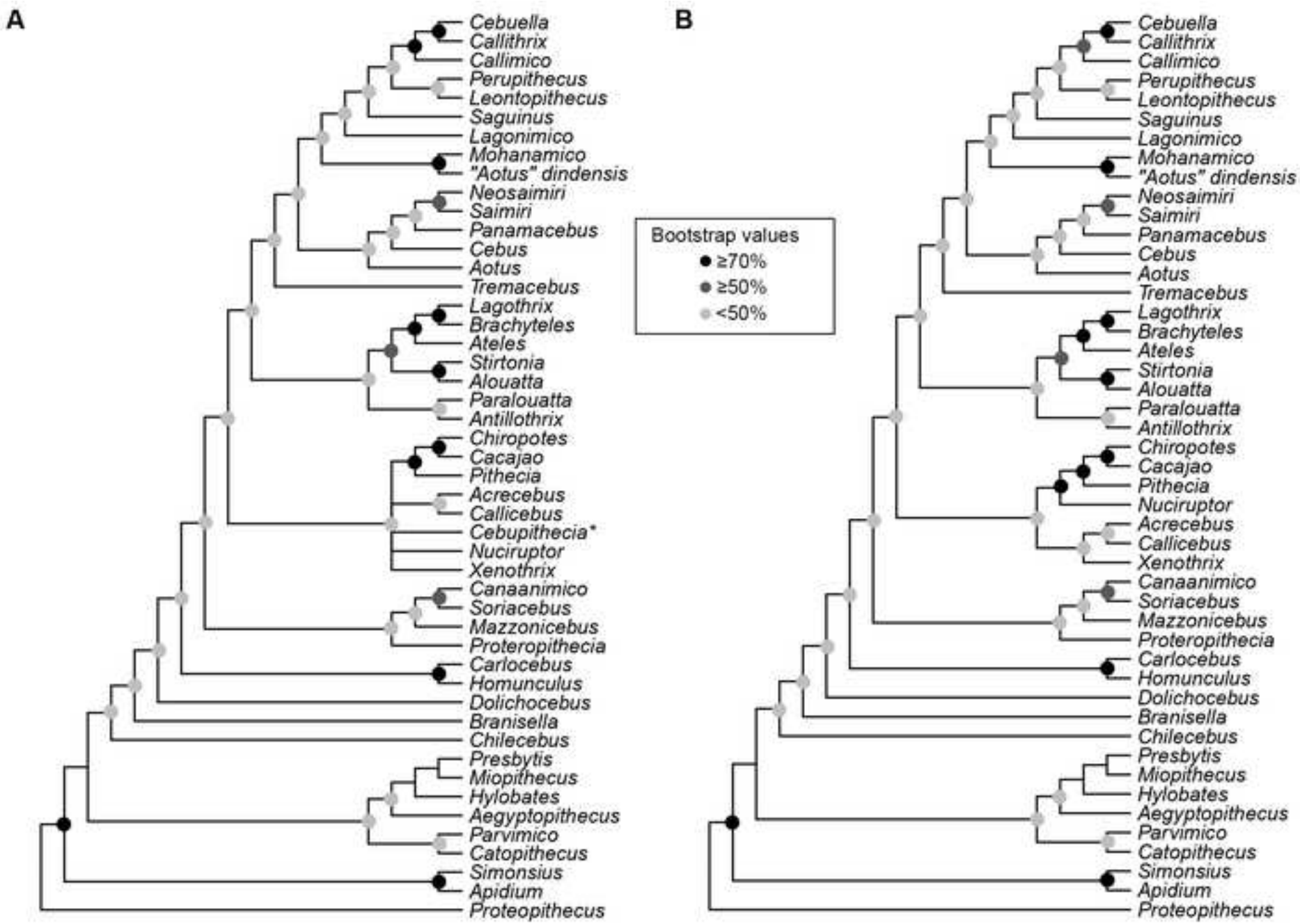

Figure 6

Click here to access/download;Figure;Fig6_TE_undated_tr_no_layers.tif

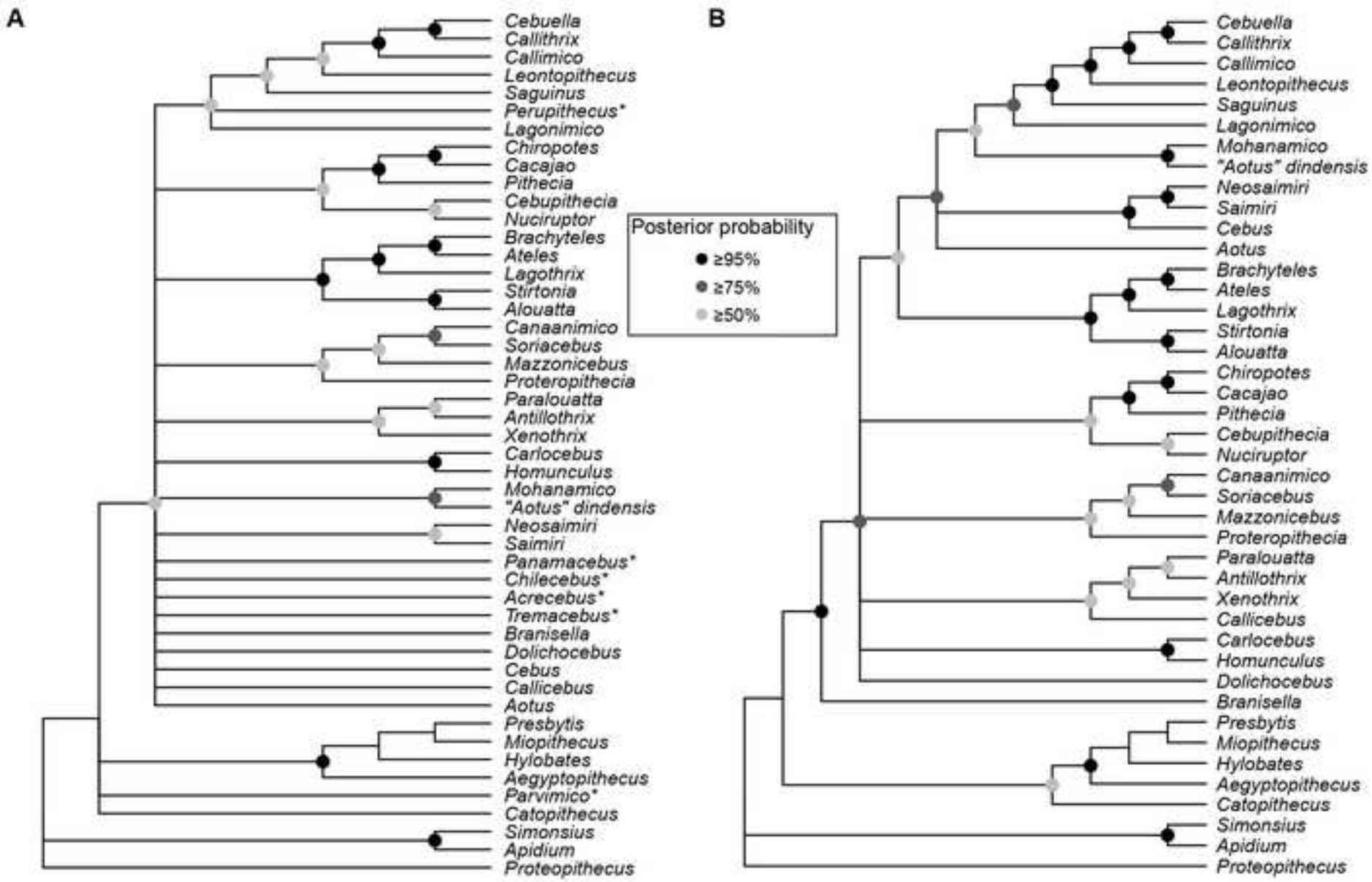

Figure 7

Click here to access/download;Figure;Fig7_TE_dated_trees_legend_dashed_no_layers.tif

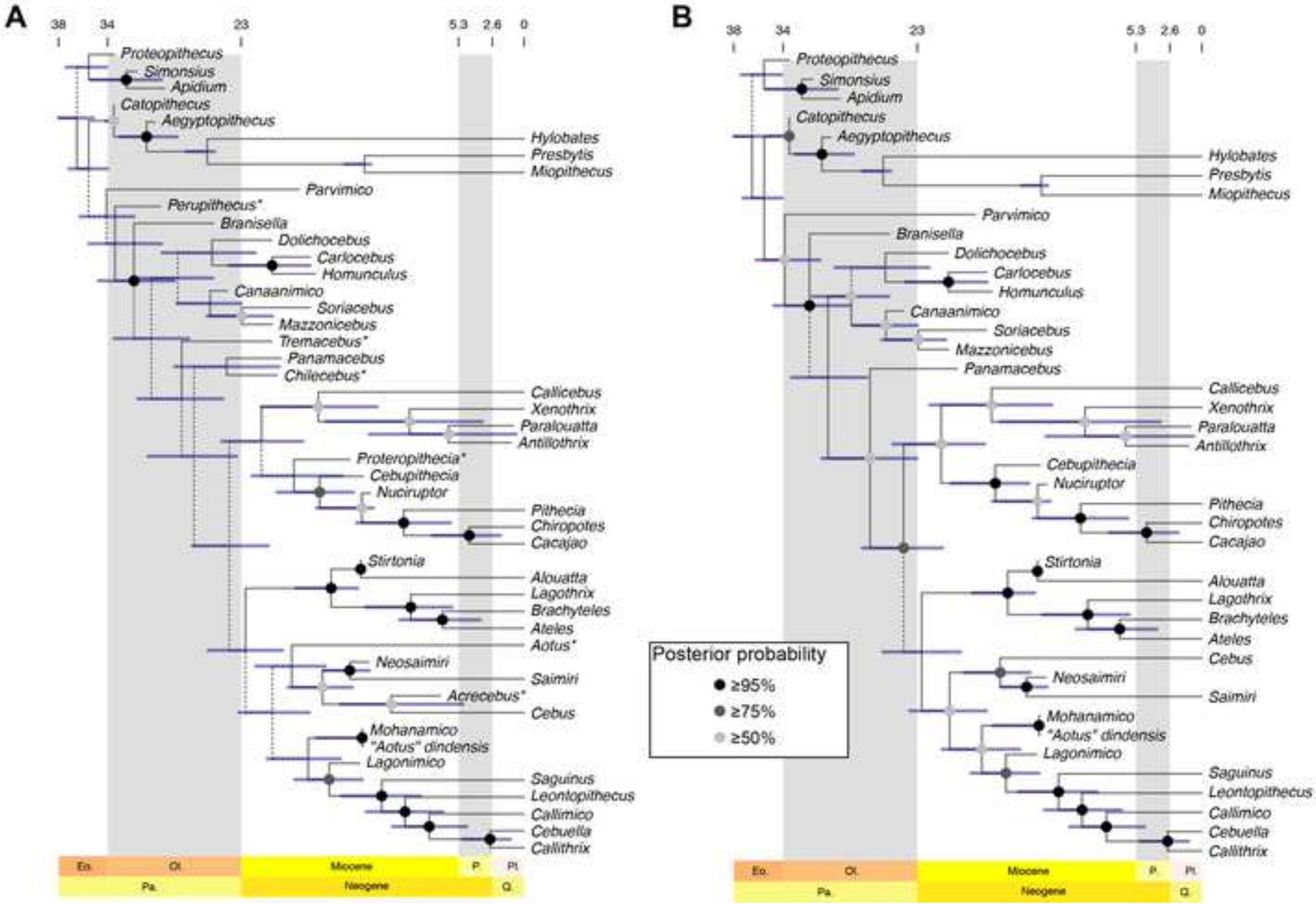

Table (Editable version)

Click here to access/download;Table (Editable version);2022-10-19-Editor accepted Tables.docx

Table 1

Molecular partitioning scheme for total evidence tip-dating analyses in MrBayes v. 3.2.7a based on PartitionFinder v. 2.2 output. Partitions were identified using the Bayesian Information Criterion for model selection and assuming linked branch lengths.

Partitions	Nuclear loci	Model[a]
1 (3307 bp)	ADORA3 (412 bp), CREM (419 bp), RPGRIP1 (677 bp), RAG1 (1071 bp), FAM123B (728 bp)	K80 + G
2 (3465 bp)	MBD5 (553 bp), RAG2 (502 bp), APP (647 bp), SGMS1 (580 bp), MAPKAP1 (644 bp), NEGR1 (539 bp)	HKY + G
3 (1105 bp)	FES (431 bp), DENND5A (674 bp)	K80 + G
4 (2367 bp)	DMRT1 (522 bp), NPAS3 (596 bp), ERC2 (713 bp), FOXG1 (536 bp)	GTR + G

bp = base pairs.

[a] G = gamma distribution to model rate heterogeneity between sites; GTR = General Time Reversible model, which assumes unequal base frequencies, and separate rate parameters for all six substitution types; HKY = Hasegawa et al. (1985) model, which assumes unequal base frequencies, and separate rate parameters for transitions and transversions; K80 = Kimura (1980) model (also known as K2P), which assumes equal base frequencies, and separate rate parameters for transitions and transversions.

Table 2

Age priors of fossil taxa used in the total evidence tip-dating analysis presented in this study (see Figure 7). All extant taxa were given a fixed age prior of 0 Ma. As recommended by Püschel et al. (2020), age priors for fossil taxa were based on the total age range of the specimen(s) used for scoring the morphological matrix of Kay et al. (2019; see also Kay, 2015), which we used as the source of our morphological data (see Methods for full details).

Fossil taxon	Age prior (uniform, unless otherwise noted)	Justification
Paralouatta	0–1.29 Ma	Described as late Quaternary based on associated fauna (Rivero and Arredondo, 1991). We use the second half of the Quaternary (Cohen et al., 2013) for this age prior.
Xenothrix	0.001443–0.001511 Ma	Radiometric date reported by Cooke et al. (2017).
Antillothrix	0.003715–1.43 Ma	The maximum bound is the maximum U-Pb date (1.32 +/- 0.11 Ma) reported by Rosenberger et al. (2015). The minimum bound is the minimum

		^{14}C date (3850 +/- 135 BP) reported by Rímoli (1977; see also Rosenberger et al., 2015).
Acrecebus	4.741–9.0 Ma	Recent age estimates for the Huayquerian SALMA include 9.0–5.28 Ma (see Prevosti and Forasiepi, 2018, table 1.1) and 9.0–6.8 Ma (Gasparini et al., 2021). However, Prevosti et al. (2021) reported a 40Ar/39Ar date from the lower 'Irenean' fauna at Quequén Salado River—which shows similarities to Huayquerian faunas—of 5.17 +/- 0.08 Ma, i.e., younger than previously proposed minimum bounds for the Huayquerian. We therefore use a more conservative minimum bound of 4.741 Ma based on the median maximum age of the Monte Hermoso fauna (Prevosti et al., 2021), which is the type fauna of the Montehermosan SALMA that follows the Huayquerian.

Proteropithecia	10.4–19.76 Ma	Known specimens of this taxon are derived from within and above the Pilcaniyeu Ignimbritic Member in the Collón Curá Formation (Kay et al., 1998a). Potassium-Argon dates ranging from 13.8 to 16.0 Ma (Marshall et al., 1977; Bondesio et al., 1980; Mazzoni and Benvenuto, 1990; Kay et al., 1998a) have been reported for the Pilcaniyeu Ignimbritic Member, as has an $^{40}Ar/^{39}Ar$ date of 15.7 Ma (Madden et al., 1997; Kay et al., 1998a), later adjusted to 15.9 Ma (Kay and Perry, 2019). However, the reliability of these dates, at least some of which are based on whole-rock samples, was questioned by Nivière et al. (2019). We therefore take a more conservative approach here. The minimum bound for this age prior is based on a 10.6 +/- 0.2 Ma U-Pb date from the overlying Caleufu Formation (López et al., 2019); the maximum bound is based on a 19.04 +/- 0.72 Ma date from $^{40}Ar/^{39}Ar$ biotite dating of the basal ignimbrite in the Collón Curá Formation (Nivière et al., 2019). This age range encompasses, but is broader than, the previously reported K-Ar and $^{40}Ar/^{39}Ar$ dates.

Neosaimiri	12.272–13.183 Ma	The type specimen of this taxon is from the Monkey Beds at La Venta, which correspond to the normal interval of Chron C5AA (Flynn et al., 1997; Kay and Madden, 1997). This interval spans from 13.183 to 13.032 Ma (Raffi et al., 2020). *Neosaimiri* specimens described by Rosenberger et al. (1991) and Takai (1994), which were also used by Kay et al. (2019) for scoring of this taxon, are from the Masato site in the "lowest part of the Tatacoa Red Member" (Takai, 1994: p. 331). According to Villarroael et al. (1996), the Tatacoa Red Member is equivalent to the El Cardon Red Beds. Magnetostratigraphic information (Flynn et al., 1997; Madden et al., 1997; Anderson et al., 2016; Montes et al., 2021) indicates that the El Cardon Red Beds are younger than the top of Chron C5Ar.2n (=12.829 Ma; Raffi et al., 2020) but older than the top of Chron C5An.2n (=12.272 Ma; Raffi et al., 2020). Therefore, the composite age range for this taxon is 12.272–13.183 Ma.

Nuciruptor	12.272–12.829 Ma	Specimens used to score this taxon for the morphological matrix used here are from the El Cardon Red Beds at La Venta (Kay, 2015). Magnetostratigraphic information (Flynn et al., 1997; Madden et al., 1997; Anderson et al., 2016; Montes et al., 2021) indicates that the El Cardon Red Beds are younger than the top of Chron C5Ar.2n (=12.829 Ma; Raffi et al., 2020) but older than the top of Chron C5An.2n (=12.272 Ma; Raffi et al., 2020).
'Aotus' dindensis	13.032–13.183 Ma	Specimens used to score this taxon for the morphological matrix used here are from the Monkey Beds at La Venta (Kay, 2015). The Monkey Beds correspond to the normal interval of Chron C5AA (Flynn et al., 1997; Kay and Madden, 1997), which spans from 13.183 to 13.032 Ma (Raffi et al., 2020).
Cebupithecia	13.032–13.183 Ma	Specimens used to score this taxon for the morphological matrix used here are from the Monkey Beds at La Venta (Kay, 2015). The Monkey Beds

		correspond to the normal interval of Chron C5AA (Flynn et al., 1997; Kay and Madden, 1997), which spans from 13.183 to 13.032 Ma (Raffi et al., 2020).
Mohanamico	13.032–13.183 Ma	Specimens used to score this taxon for the morphological matrix used here are from the Monkey Beds at La Venta (Kay, 2015). The Monkey Beds correspond to the normal interval of Chron C5AA (Flynn et al., 1997; Kay and Madden, 1997), which spans from 13.183 to 13.032 Ma (Raffi et al., 2020).
Stirtonia spp.	13.032–13.608 Ma	The older species used by Kay (2015) for scoring purposes, namely *Stirtonia victoriae*, is from Duke Locality 28 at La Venta, within the Cerro Gordo Beds of the La Victoria Formation, which lies within Chron C5ABn (Flynn et al., 1997; Madden et al., 1997; Anderson et al., 2016; Montes et al., 2021); this spans from 13.608–13.363 Ma (Raffi et al., 2020), with the latter date providing our minimum bound. The younger species used by

		Kay (2015) for scoring purposes, namely *Stirtonia tatacoensis*, is from the Monkey Beds and Fish Beds, which are older than the minimum age of Chron C5AAn (Flynn et al., 1997; Madden et al., 1997; Anderson et al., 2016; Montes et al., 2021), which is 13.032 Ma (Raffi et al., 2020).
Lagonimico	13.183–13.608 Ma	Date for Duke/INGEOMINAS locality 90, source of the holotype of *Lagonimico conclucatus* (de Vries and Beck, 2021[a]; Montes et al., 2021).
Homunculus spp.	16.29–17.668 Ma	All of the *Homunculus* specimens appear to be from Santacrucian sites on the Atlantic coastal plain (see Appendix 16.1 of Kay et al., 2012), which Perkins et al. (2012) dated to 18–16 Ma. More recently, Trayler et al. (2021) presented a revised age model for six Santa Cruz localities on the Atlantic coastal plain; this indicates a minimum bound of 16.55–0.26 (=16.29) Ma and a maximum bound of 17.613 + 0.055 (=17.668) Ma, based on the 95% highest posterior interval for their summed probability distribution likelihood model (Trayler et al., 2021, table 2).

Parvimico	16.4–19.6 Ma	Radiometric date reported by Kay et al. (2019).
Carlocebus spp.	16.761–18.01 Ma	*Carlocebus* spp. are from the Pinturas Formation, which is overlain by the Toba Blanca tuff (Perkins et al., 2012). According to Trayler et al. (2020, table 2), the 95% highest density interval model age of the Toba Blanca tuff is 16.806 + 0.039/- 0.045 Ma, which provides a minimum bound of 16.761 Ma. Perkins et al. (2012) gave a date from near the base of the formation at the Estancia El Carmen is 17.99 +/- 0.02 Ma, which we use as a maximum of 18.01 Ma.
Soriacebus spp.	16.761–18.01 Ma	*Soriacebus* is from the Pinturas Formation, which is overlain by the Toba Blanca tuff (Perkins et al., 2012). According to Trayler et al. (2020, table 2), the 95% highest density interval model age of the Toba Blanca tuff is 16.806 + 0.039/- 0.045 Ma, which provides a minimum bound of 16.761 Ma. Perkins et al. (2012) gave a date from near the base of the formation at the Estancia El Carmen is 17.99 +/- 0.02 Ma, which we use as a maximum

		of 18.01 Ma.
Panamacebus	18.636–21.1 Ma	The overlying Centenario Fauna is within C5Er (MacFadden et al., 2014), which is 18.636–18.497 Ma according to Raffi et al. (2020); 18.636 Ma is therefore the minimum bound for this age prior. The maximum bound is the maximum age of the radiometric date underlying the fossil deposit, as presented by Bloch et al. (2016).
Chilecebus	19.82–20.36 Ma	Radiometric date reported by Flynn et al. (1995).
Mazzonicebus	19.979–21.130 Ma	Material came from the Colhue-Huapi West locality, the Lower Fossil Zone (LFZ) of the Colhue-Huapi Member, Sarmiento Formation at Gran Barranca (Kay, 2010). The LFZ corresponds to Chron C6An.1n according to Ré et al. (2010), which is 20.182–19.979 Ma (Raffi et al., 2020). However, according to Dunn et al. (2013), the LFZ spans C6An.2r to C6An.2n, which is 21.130 to 20.448 Ma following Gradstein et al. (2012).

		We use the maximum possible age range for this age estimate here.
Dolichocebus	20.1–21.0 Ma	Material comes from the Trelew Member of the Sarmiento Formation which belongs to the Colhuehuapian SALMA (Kay et al., 2008). We follow the age estimate for the Colhuehuapian SALMA of Dunn et al. (2013).
Tremacebus	20.1–21.0 Ma	Materials come from Colhuehuapian aged deposits at approximately 12 km southwest of Cerro Sacanana, in north central Chubut (Hershkovitz, 1974). We follow the age estimate for the Colhuehuapian SALMA of Dunn et al. (2013).
Canaanimico	23–26.63 Ma	The minimum bound is provided by the minimum age of the Deseadan SALMA (Dunn et al., 2013). The maximum bound is based on the underlying, dated tuff that is ~5m below the fossils (Marivaux et al., 2016).
Branisella	25.264–25.304 Ma	Kay et al. (1998b) correlated the 'Branisella Zone/Level' (=Unit 5) at Salla to C8n.lr; according to Speijer et al. (2020), this is 25.304–25.264 Ma.

Perupithecus	29.52–29.68 Ma	Radiometric date reported by Campbell et al. (2021).
Aegyptopithecus	28.2–33.4 Ma	Most specimens of the only known species of *Aegyptopithecus*, *Aegyptopithecus zeuxi*, appear to be from 'Quarry M', which is one of the youngest sites in the Gebel Qatrani Formation (Seiffert, 2006, 2010; Seiffert et al., 2010). However, *A. zeuxi* has also been reported from the older 'Quarry I' (Seiffert et al., 2010), which has been estimated to be 29.8–30.0 Ma (Gunnell et al., 2010, table 7.1; Gunnell, 2010, table 30.1), and the age of the Gebel Qatrani Formation itself is somewhat controversial (see Van Couvering and Delson, 2020). Thus, we assign an age representing the entirety of the 'Qatranian' (sensu Van Couvering and Delson, 2020), which is 33.4–28.2 Ma.
Apidium	28.2–33.4 Ma	*Apidium* spp. are known from multiple quarries in the Gebel Qatrani Formation (Seiffert et al., 2010). We therefore assign an age representing the entirety of the 'Qatranian' (sensu Van Couvering and Delson, 2020),

		which is 33.4–28.2 Ma.
Simonsius	28.2–33.4 Ma	Similar to *Aegyptopithecus*, *Simonsius* (=*Parapithecus*) *grangeri* is known from Quarry M and Quarry I in the Gebel Qatrani Formation (Seiffert et al., 2010). We therefore assign an age representing the entirety of the 'Qatranian' (sensu Van Couvering and Delson, 2020), which is 33.4–28.2 Ma.
Catopithecus	33.4 Ma (fixed)	This taxon is from Quarry L-41 in the Fayum Depression, Egypt. The age of this site has been subject to different interpretations (Gingerich, 1993; Seiffert, 2006, 2010; Van Couvering and Delson, 2020). It was most recently reviewed by Van Couvering and Delson (2020: p. 12), who stated that “the reversed polarity of the uppermost Qasr el-Sagha and that of the lowermost Gebel Qatrani (Rasmussen et al., 1992) could be a composite of the C15r reversal below and the C13r reversal above the Eocene-Oligocene boundary”, and assigned an age of 33.4 Ma to this site, in contrast to the

		slightly older (~34 Ma) age preferred by Seiffert (2006, 2010). We follow Van Couvering and Delson's (2020) proposed age, which we use as a fixed age estimate for this site, but note that the site may be slightly older than this, as argued by Seiffert (2006, 2010).
Proteopithecus	33.4 Ma (fixed)	This taxon is from Quarry L-41 in the Fayum Depression, Egypt. We follow Van Couvering and Delson's (2020) proposed age of 33.4 Ma, which we use as a fixed age estimate for this site, but we note that this site may be slightly older (~34 Ma; Seiffert, 2006, 2010).

[a] *bioRxiv* preprint (not yet accepted for publication by a peer-reviewed journal)

Table 3

Taxa identified as unstable in each phylogenetic analysis, based on the 'splitwise phylogenetic information content' with a threshold of 50 (corresponding to a 50% majority rule consensus), as implemented by the R package Rogue v. 2.1.0. Taxa are ranked from most unstable to least unstable. Percentage completeness for the morphological dataset, and corresponding rank of completeness (out of a total of 48 taxa) are given in parentheses.

Molecular, Bayesian undated	Morphology, MP	Morphology, Bayesian undated	Morphology with molecular scaffold, MP	Morphology with molecular scaffold, Bayesian	Total evidence, Bayesian undated	Total evidence, Bayesian tip dating
(None)	(None)	1. *Proteropithecia* (14.8% complete; 44/48) 2. *Xenothrix* (43.5% complete; 34/48) 3. *Tremacebus* (21.3% complete; 42/48) 4. *Perupithecus* (9.3% complete; 48/48)	1. *Cebupithecia* (51.4% complete; 30/48)	1. *Chilecebus* (21.1% complete; 43/48) 2. *Perupithecus* (9.3% complete; 47/48) 3. *Proteropithecia* (14.8% complete; 44/48) 4. *Tremacebus* (21.3%; 42/48)	1. *Perupithecus* (9.3% complete; 47/48) 2. *Parvimico* (9.1% complete; 48/48) 3. *Chilecebus* (21.1% complete; 43/48) 4. *Acrecebus* (9.6% complete; 46/48)	1. *Proteropithecia* (14.8% complete; 44/48) 2. *Tremacebus* (21.3% complete; 42/48) 3. *Acrecebus* (9.6% complete; 46/48) 4. *Perupithecus* (9.3% complete; 47/48)

	5. *Parvimico* (9.1% complete; 48/48) 6. *Chilecebus* (21.1% complete; 43/48) 7. *Panamacebus* (22.0% complete; 41/48)	5. *Acrecebus* (9.6% complete; 46/48)	5. *Tremacebus* (21.3% complete; 42/48) 6. *Panamacebus* (22.0% complete; 41/48)	5. *Aotus* (91.1% complete; 3/48) 6. *Chilecebus* (21.1% complete; 43/48)

MP = maximum parsimony.

Table 4

Divergence dates estimated for selected clades in our total evidence tip-dating analysis, prior to pruning of unstable taxa (see Fig. 4A). Values are median posterior estimates, followed by 95% highest posterior density intervals in parentheses.

Clade	Split	Estimated divergence time (Ma)
Crown Anthropoidea	Catarrhini-Platyrrhini	35.4 (33.9–37.1)
Crown Platyrrhini	Pitheciidae-(Aotidae + Atelidae + Callitrichidae + Cebidae)	24.0 (20.8–27.0)
Crown Pitheciidae	Pitheciinae-Callicebinae	21.4 (18.0–24.6)
Crown Pitheciinae	*Pithecia*-(*Chiropotes* + *Cacajao*)	9.8 (6.0–13.6)
Callicebus + Greater Antillean platyrrhines	*Callicebus*-(*Xenothrix* + *Antillothrix* + *Paralouatta*)	16.8 (12.0–21.4)
Greater Antillean platyrrhines	*Xenothrix*-(*Antillothrix* + *Paralouatta*)	9.3 (3.4–16.1)
Atelidae + Aotidae + Callitrichidae + Cebidae	Atelidae-(Aotidae + Callitrichidae + Cebidae)	22.7 (19.7–25.7)
Crown Atelidae	Alouattinae-Atelinae	15.7 (13.5–18.6)
Crown Atelinae	*Lagothrix*-(*Brachyteles* + *Ateles*)	9.2 (5.9–12.9)
Crown Callitrichidae	*Saguinus*-(*Leontopithecus* + *Cebuella* + *Callithrix* + *Callimico*)	11.6 (8.4–14.9)
Crown Cebidae	Cebinae-Saimirinae	16.4 (14.0–19.2)